A STUDY OF

ELECTRO-MAGNETIC TRANSITIONS

IN ^{38}Ca

by

Edward C. Hagen

Date: April 1974

Approved:

_____

N.R.Roberson, Supervisor

_____

_____

_____

_____

A dissertation submitted in partial fulfillment of the requirements for the degree of Doctor of Philosophy in the Department of Physics in the Graduate School of Arts and Sciences of Duke University

1974

ABSTRACT

(Physics)

A STUDY OF ELECTRO-MAGNETIC TRANSITIONS IN ^{38}Ca

by

Edward C. Hagen

Date: _____

Approved:

_____

N.R. Roberson, Supervisor

_____

_____

_____

_____

A dissertation submitted in partial fulfillment of the requirements for the degree of Doctor of Philosophy in the Department of Physics in the Graduate School of Arts and Sciences of Duke University

1974

A STUDY OF

ELECTRO-MAGNETIC TRANSITIONS

IN ^{38}Ca

by

Edward Christopher Hagen

The Doppler shift attenuation method (DSAM) has been used to measure the mean lifetimes of low-lying excited states of ^{38}Ca. The levels were populated by the $^{36}Ar(^{3}He,n\gamma)^{38}Ca$ reaction at ^{3}He bombarding energies of 9.0, 10.0 and 10.5 MeV. Both enriched (99.6%) ^{36}Ar gas and solid targets were used. The solid target was a tantalum foil with ^{36}Ar embedded in it. Precise energies for the first six levels have been determined. A doublet at 3.7 MeV was resolved as a $J^{\pi} = 3^{-}$ state at 3.703 MeV and a $J^{\pi} = 2^{+}$ state at 3.684 MeV. The lifetimes determined in this study are $98\pm^{44}_{40}$ fs, $27\pm^{17}_{11}$ ps, <8 fs, $225\pm^{100}_{85}$ fs and 35 ± 17 fs for the levels at 2.213, 3.084, 3.684, 3.703 and 4.384 MeV. The lifetime of the level at 4.193 MeV was not determined.

The experimental level scheme is compared with other A = 38 nuclei and with a calculation performed with the Oak Ridge-Rochester shell model code. The model used $(s_{1/2})^{j}(d_{3/2})^{k}(f_{7/2})^{l}(p_{3/2})^{m}$ configurations with $1 + m \leq 2$, $j \geq 2$ and $k \geq 4$.

ACKNOWLEDGEMENTS

I wish to express my gratitude to Dr. N. R. Roberson who has given his interest and support to his project. His suggestions have improved the quality of this work. I would like to thank Dr. D. R. Tilley for many helpful discussions related to both the experimental techniques and the analysis of the data. The assistance of Mr. J. D. Hutton is deeply appreciated. Thanks are due Drs. R. Bass and W. Kessel for the loan of the gas cell. Thanks are due Drs. C. R. Gould and R. O. Nelson for their aid in computer programming. I would like to thank Mr. S. E. Edwards for his rapid aid with the electronics and Mr R. L. Rummel and M. T. Smith for their help with the accelerator. Thanks are due to Mr. A. W. Lovette, Mr. E. P. Harris and Mr. R. G. Hogan for the excellant machine work they performed.

I would like to thank Dr. S. Maripuu for his help with the shell model program. I would like to express my gratitude to Dr. H. W. Newson and the TUNL staff for providing me with the research assistantship. I wish to thank my family for their support and encouragement during my graduate education. Most of all I wish to thank my wife Sally for her unfailing support, good humor and common sense.

This work was supported in part by the U. S. Atomic Energy Commission.

E. C. H.

CONTENTS

LIST OF FIGURES

LIST OF TABLES

A STUDY OF

ELECTRO-MAGNETIC TRANSITIONS

IN ^{38}Ca

Chapter 1

INTRODUCTION

A. General

Nuclei near closed shells are attractive subjects for experimental and theoretical investigation because they can be represented by a single particle (hole) or pair of particles (holes) outside an inert core. However, neither calculations with this simple model, nor shell model calculations with larger but still restricted configuration spaces (Engelbertink 1970, Glaudemans 1971, Skouras 1969, Wildenthal 1968,1971) have had complete success describing the details of the nuclei in this region. Full shell model calculations, having many more active nucleons, are much more difficult computationally, due to the large size of the matrices that must be diagonalized. For example, the Oak Ridge-Rochester shell model program can process matrices as large as 537x537. If the full basis of the Pauli allowed states has to be truncated to fit this restriction, significant errors can be introduced. Thus comparison with experimental results are of practical interest to determine the size necessary to attain accurate predictions. As is pointed out by Halbert et.al. a comparison of excitation energies, spectroscopic factors and transition strengths (mean lifetimes) from a restricted model with the experimental data can help determine whether the model can be applied with any confidence.

The nuclei near the doubly magic (N=Z=20) ^{40}Ca have been extensively studied. The mirror nuclei ^{39}K and ^{39}Ca, which can be represented as a $(d_{3/2})$ hole in a ^{40}Ca core have recently been studied by Kessel, et.al.(1973,1974). While the A = 38 nuclei ^{38}K and ^{38}Ar have been the subjects of extensive experimental investigation (Engmann 1971, Hasper 1973, Engelbertink 1969), the mirror nucleus of ^{38}Ar, ^{38}Ca, is not as well known.

B. Methods of Measuring Nuclear Lifetimes

The mean lifetimes of excited nuclear states range from days in the case of isomeric states to less than 10^{-15} seconds. Since no one experimental technique has the latitude necessary to cover this broad range, many different techniques have evolved. The more successful of these are listed in Table 1. The lifetime of a level is related to the total width Γ by the relation $\Gamma = h/\tau$, where τ is the mean lifetime. Both resonance fluorescense and coulomb excitation have the advantage that they measure widths directly, but suffer the drawback that the target must be composed of the nuclide being studied, thus limiting their use to the study of the characteristics of stable nuclei. The recoil distance method and the Doppler shift attenuation method use charged particle induced reactions to populate the states to be studied, so that any nucleus that is accessible to the reaction is available for study. Since the lifetimes of low-lying bound states of nuclei in the s-d shell are usually in the pico- to femto-second range, the RDM and the DSAM are the most applicable. Both of these methods rely on the Doppler effect.

The recoil distance method uses the Doppler effect to distinguish between those recoiling nuclei that decay in flight and those that have come to rest before decaying. Using a movable stopper, the distance of flight is varied, and the ratio of stopped to unstopped nuclei measured. Because the velocity is determined by the reaction kinematics, the recoiling nuclei take a known time to traverse the vacuum between the target and the stopper. A series of measurements can determine the mean lifetime of the excited state of interest.

Table I

Methods of Measuring Mean Lives

and the Range of Their Applicability

Method	Range of Mean Lifetimes (sec)
Electronic Timing	$\tau > 10^{-10}$
Recoil Distance (RDM)	$10^{-12} < \tau < 5 \times 10^{-9}$
Doppler Shift Attenuation (DSAM)	$5 \times 10^{-15} < \tau < 10^{-11}$
Resonance Fluorescence [a)]	$\tau < 10^{-10}$
Coulomb Excitation [a)]	$10^{-15} < \tau < 10^{-8}$

a) Bashandy 1961

The Doppler shift attenuation method, instead of distinguishing between stopped and unstopped nuclei, determines the velocity at which an excited nucleus decays as it slows down in matter. If the slowing down time of the recoiling nucleus is on the order of the lifetime to be measured, the instantaneous velocity will be less than the initial velocity, but greater than zero. Thus the observed Doppler shift will be attenuated by an amount proportional to the ratio of the instantaneous to initial velocities.

The observed energy, E_γ, of the γ-ray emitted by a moving source is given by

$$E_\gamma = E_{\gamma 0}(1 + \frac{v(t)}{c} \cos(\Psi_\gamma))$$

where $E_{\gamma 0}$ is the energy of the γ-ray when the nucleus is at rest, $v(t)$ is the instantaneous velocity, and Ψ is the angle between the direction of motion and the observer. The percentage shift is given by

$$\frac{E_\gamma - E_{\gamma 0}}{E_{\gamma 0}} = \frac{v(t)}{c} \cos(\Psi_\gamma)$$

To observe such a shift with a NaI detector having an energy resolution of >6%, the velocity of the recoiling nucleus must be greater than 6% of the velocity of light. Such velocities are not usually attained in nuclear reactions except for the special case of heavy ion induced reactions. This fact places a severe limit on the number of nuclear levels available for investigation. However, Devons, et.al. were able to demonstrate the practicality of the method in their pioneering work of 1954.

With the advent of the lithium-drifted germanium diode (Ge(Li)) as a detector of muclear radiation with energy resolutions of ≈0.15%, the Doppler shift attenuation has become a standard tool for the study of nuclear spectroscopy. With charged particle reactions such as (^{3}He,n)

the maximum Doppler shifts predicted by the reaction kinematics, i.e. the shifts that would be seen at t=0, are in general greater than the typical detector resolution. The ratio of the observed shift to the maximum shift is the attenuation factor $F(\tau)$. For a γ-ray observed at an angle θ_γ, with respect to the beam axis, the observed Doppler shift is expressed by

$$\Delta E_\gamma (t) = E_\gamma(t) - E_{\gamma 0} = E_{\gamma 0}\frac{v(t)}{c}\cos(\theta_\gamma + \phi(t))$$

where $\phi(t)$ is the angle between the beam axis and the instantaneous velocity and $\Psi = \theta_\gamma + \phi$. Since the scattering that changes the direction of the recoiling nucleus is symmetric about the initial direction and since

$$\cos(\theta + \phi) = \cos(\theta)\cos(\phi) - \sin(\theta)\sin(\phi),$$

the energy of a group of recoiling nuclei (averaging about the recoil axis), will contain the cosine terms only, and the attenuation factor for this group of nuclei which decays at time t will be

$$F(\tau) = \frac{\overline{v(t)\cos\phi(t)}}{v(0)}$$

The attenuation factor for an ensemble of nuclei created at t = 0 is thus

$$F(\tau) = \frac{\int F(t)R(t)dt}{\int R(t)dt}$$

where $R(t) = dN/dt$ is the decay rate of the nuclei. For radioactive nuclei this is determined from

$$N(t) = N(0)e^{-t/\tau}$$

where τ is the mean lifetime. The attenuation factor is then

$$F(\tau) = \frac{1}{\tau v(0)} \int \overline{v(t)\cos(\phi(t))} e^{-t/\tau} dt$$

Ions recoiling in matter lose energy to atomic electrons through ionization and excitation and to other nuclei through collisions. While the nuclear part of the energy loss is discontinuous and is characterized by changes in direction as well as velocity, the electronic part of the energy loss is relatively smooth, and for velocities below $(c/137)Z^{2/3}$ is approximately proportional to the velocity of the recoiling ion (LSS 1963, LS 1961). The energy loss has the form

$$\frac{dE}{dx} = k_e \frac{dE}{dx_e} + k_n \frac{dE}{dx_n}$$

To calculate an attenuation factor $F(\tau)$ for a given τ and $v(0)$ using the formula

$$F(\tau) = \frac{1}{\tau v(0)} \int_0^\infty v(t)\cos(\Psi(t))\ e^{-t/\tau} dt$$

it is necessary to know the average of $v(t)\cos(\Psi(t))$.

Lindhard, et.al. have derived expressions for the electronic and nuclear part of the stopping power. Their predictions agree well with experimental data over a wide range of stopping materials and recoiling ions. An oscillation of the electronic part of the stopping power with increasing mass of the recoiling ions has been observed by Ormrod, et.al. and Fastrup, et.al. These oscillations can easily be accounted for in the calculations by varying the proportionality constant k_e in accordance with the experimental data.

Blaugrund has derived equations for the velocity of a scattering ion and has obtained an expression for the average $\overline{\cos(\Psi(t))}$. He notes

that the product of the average velocity and the average cosine differs at most by 10% (when the atomic numbers of the ion and substrate are the same) from the average of the product $v(t)\overline{\cos(\Psi(t))}$.

The program FTAU (Ragan 1970) uses the theoretical expressions of LSS for the stopping power and the Blaugrund approximation for the time dependence of $\overline{v(t)\cos(\Psi(t))}$ to calculate a table of attenuation factors and lifetimes.

C. Objectives of the Present Study

While information on the lifetimes of excited states has increased enormously in recent years, accurate experimental information for the low-lying levels of proton rich nuclei is still relatively less complete than for neutron rich nuclei. The (^{4}He,n), (^{3}He,n) and (p,t) reactions have emerged as useful tools for the study of the proton rich nuclei.

The mass 38 nuclei argon and potassium have been the subject of extensive investigation (Hasper 1973, Engmann 1971, Engelbertink 1969) whereas the properties of ^{38}Ca are less well known. These three nuclei are members of a T = 1 isobaric triad. Knowledge of the strengths of corresponding transitions in all three members of a triad can allow the unambiguous determination of the isoscaler and isovector parts of the transition matrix elements(Warburton 1969). The electromagnetic strength of the 2.2 MeV transitions from the T = 1, $J^\pi = 2^+$ state to the T = 1, $J^\pi = 0^+$ ground state in ^{38}Ar has been measured with precision (Englebertink 1969) and the corresponding transition in ^{38}K has been the subject of several recent studies (Engmann 1971, Hasper 1973). No transition strengths have yet been measured for ^{38}Ca.

Accurate determination of the level energies is needed to supple-

ment the work of Shapiro,et.al. and Davies,et.al. who studied the $^{36}Ar(^{3}He,n)$ and $^{40}Ca(p,t)$ reactions, respectively. The knowledge of transition strengths for the gamma decays of the excited states is necessary to further the study of this interesting triad.

Chapter II

EXPERIMENTAL EQUIPMENT

A. General

The states in ^{38}Ca were populated via the $^{36}Ar(^{3}He,n\gamma)^{38}Ca$ reaction. The neutrons were detected in coincidence with the γ-rays emanating from excited states in ^{38}Ca. Coincident techniques are necessary if there are many different reactions open for the particular beam energy and target combination, or if the background radiation competes successfully with the radiation from the decays of the excited states in the nucleus of interest. Detection of the neutrons also has the advantage that it defines the direction and magnitude of the velocity of the recoiling nuclei. The knowledge of the direction of the velocity of the recoiling nuclei removes the uncertainty of determining the average recoil velocity of the excited nuclei whose angular distribution is usually unknown.

B. The ^{3}He Beam

The TUNL duoplasmatron negative ion source provided 100 - 700 nA beams of He^{-} which were accelerated to the desired energy by the TUNL model FN Tandem van de Graaff accelerator. The negative ions were accelerated to the high voltage terminal at the center of the machine where they passed through a region containing oxygen gas. Collisions with

the gas removed electrons from the $^3He^-$ ions. The resulting $^3He^+$ and $^3He^{++}$ ion beams were then accelerated to the final energy. An analyzing magnet and quadrupole system was used to focus the $^3He^{++}$ beam onto the target. Typical beam currents on target were between 10 and 150 nA.

C. Target Chambers

The two target chambers used in this study are shown in Figure 1. Part (a) shows the gas cell which held isotopically enriched ^{36}Ar (99.9%) gas at pressures up to 6 atmospheres. The ^3He beam entered the cell containing the argon gas by passing through a 10.6 mg/cm tantalum foil. In order to minimize background radiation, both chambers were constructed in such a way that the beam could only strike defining collimators or the target. The ratio of target current to collimator current was kept greater than 50:1. The glass chamber was pumped with a Vac-Ion pump which produced pressures less than 8×10^{-7} Torr. The gas cell was evacuated to a pressure of less than 4×10^{-6} Torr before the ^{36}Ar gas was bled into the cell. The ^{36}Ar gas could be recaptured into the storage cylinder by cooling the cylinder with liquid nitrogen, thus condensing the gas.

D. Target Preparation

The gas cell with its low densities allowed measurements of lifetimes as short as 1 ps. In order to measure mean lifetimes in the range of 10 fs. to 1 ps. a denser target, i.e. one that had stopping times in the same range, was necessary. The method of freezing argon on a metal surface cooled by liquid helium was not used, primarily due to the difficulty of construction, but also due to the problem of localized heat-

Figure 1. The two target chambers used in this work are shown along with the γ-ray and neutron detectors. The chamber shown in part a) is glass and is used to hold solid foil targets. Part b) shows the gas target and collimators.

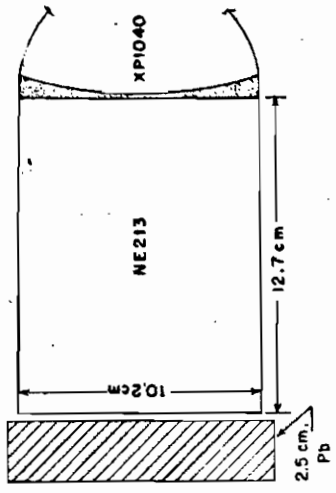
XP1040
NE213
12.7 cm
10.2 cm
2.5 cm Pb

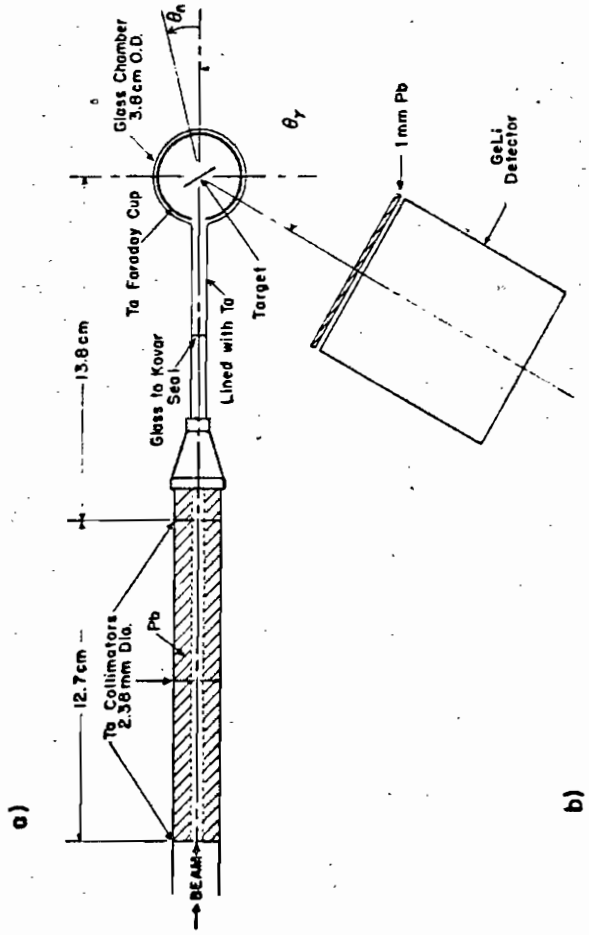
a)
Glass Chamber 3.8 cm O.D.
θ_n
θ_γ
1 mm Pb
GeLi Detector
To Faraday Cup
Target
Lined with Ta
Glass to Kovar Seal
13.8 cm
12.7 cm
To Collimators 2.38 mm Dia.
Pb
BEAM
b)
Movable Ta Stopper
Pressure Gauge
To Entrance Foil
To Collimators
Valves
Storage Cylinder
Teflon Insulator
Brass Extension Tube

ing by the beam, which would vary the target thickness. The method used in this experiment was to implant argon in a metal foil.

Preliminary work with ion-implantation was done with natural argon beams accelerated to 1 MeV with the Duke University 4 MV van de Graaff accelerator. The natural argon was implanted in foils of silver, carbon, and tantalum. Only the tantalum offered the combination of high saturability, good structural strength and high stopping power. At the start of this preliminary work, tests were made to determine if the van de Graaff and magnetic analyzer could be used as an isotope separator. Figure 2 shows a beam profile for a terminal potential of 2 MV. Because the residual gas in the accelerator tube exchanged electrons with the beam ions the energy of the beam was not well defined and the large ^{40}Ar beam was spread into the region of the ^{36}Ar (0.3% natural abundance) beam. It was therefore necessary to accelerate isotopically enriched and chemically pure ^{36}Ar gas during the manufacture of the ion-implanted target.

The target used in this study was made by accelerating the pure ^{36}Ar from an energy of 500 keV to 2200 keV in steps of 33 keV. At each energy the total integrated beam current was kept constant at a value corresponding to the saturation value of argon in tantalum (Selin 1967). The beam was kept defocused and the current adjusted to limit the power dissipated by the target to less than 5 watts/cm^2. The areal density of the ion-implanted target was estimated to be $\sim$600 μg/cm^2 on the basis of the total integrated charge and the average beam spot size. However, since the focusing property of the accelerator was a strong function of the beam energy, the estimate of the beam spot size and thus the density were uncertain. The thickness of the target was measured by comparing the γ-ray yield from the $^{36}Ar(^{3}He,n\gamma)^{38}Ca$ reaction in the foil to the yield from the

Figure 2. Natural argon beam current versus field strength as measured in the analyzing magnet of the 4 MV accelerator. Arrows indicate calculated fields for $^{40}Ar^{+}$ and $^{36}Ar^{+}$. The energy of the beam was 2 MV.

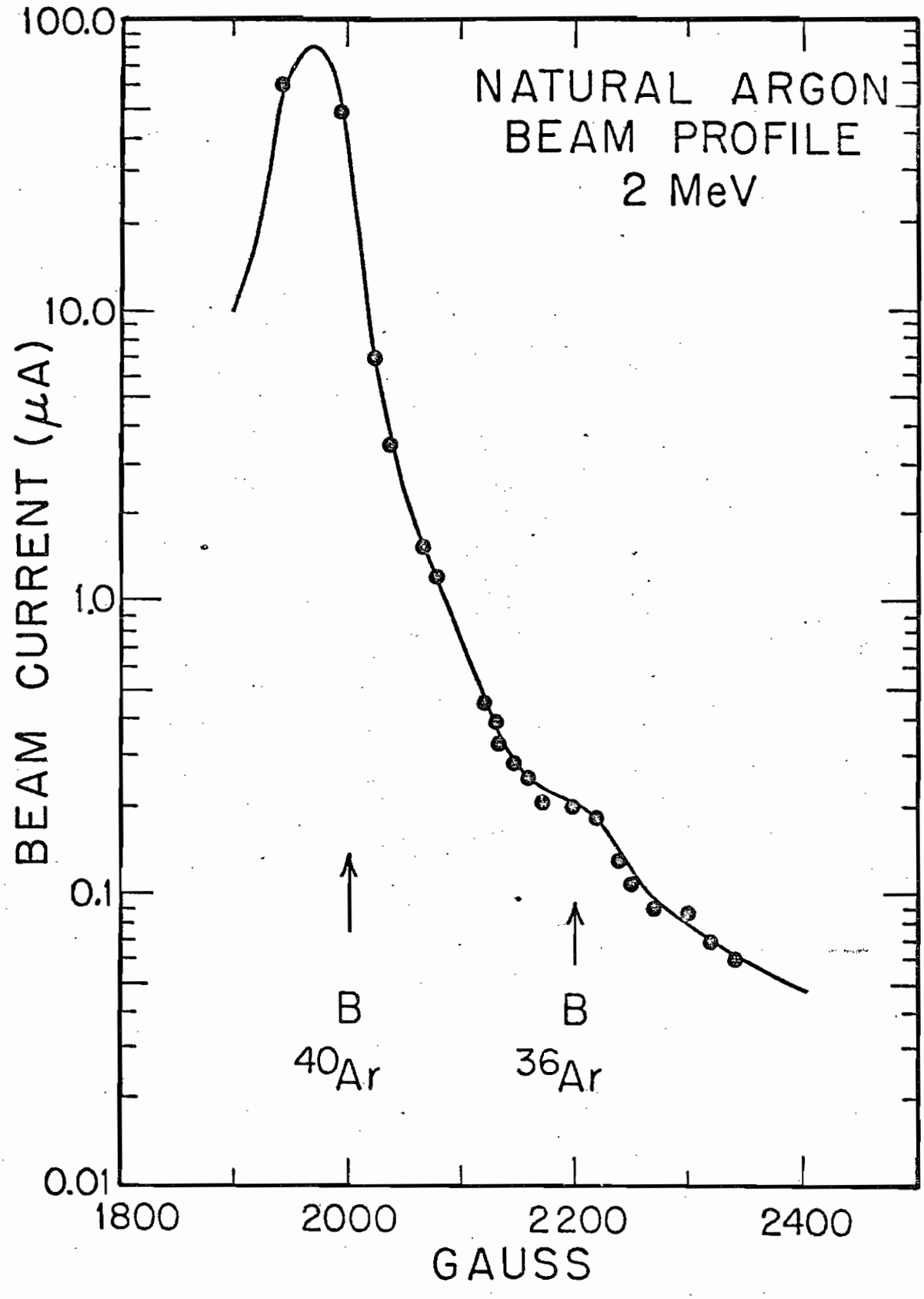
NATURAL ARGON
BEAM PROFILE
2 MeV
100.0
10.0
1.0
0.1
0.01
BEAM CURRENT (μA)
B
40Ar
B
36Ar
1800
2000
2200
2400
GAUSS

reaction in the gas cell. This measurement indicated a thickness of ∿300 μg/cm . Knowledge of the amount of argon in the tantalum foil is not sufficient to determine lifetimes using the DSAM. Since the ^{3}He beam loses energy in the foil, it creates an ensemble of recoiling nuclei with differing initial recoil velocities. Thus it is necessary to determine the spatial distribution of the argon in the tantalum.

To determine this distribution the $^{36}Ar(p,\gamma)^{37}K$ reaction was employed. An isolated proton capture resonance is located at a proton energy of 0.918 MeV and has a width of 0.8 keV (Arnell 1963). The reaction populates the fifth excited state in ^{37}K at 2.75 MeV which decays by γ-ray emission to the ground state. The homogenized proton beam (Parks 1958) from the Duke University 3 MV accelerator was varied in energy from 0.920 to 1.050 MeV. As the proton beam was stepped in energy, it had to penetrate further into the foil before it lost enough energy to be at the resonance energy. Since the resonance width was small relative to the energy loss in the foil, a measurement of the yield of the reaction was also a measure of the relative density of the argon in a specific layer.

The 2.75 MeV γ-rays from the decays of the ^{37}K were detected in a 10.2 x 12.5 cm NaI crystal. Runs of 30 minutes duration were taken at each 5 keV step in beam energy. Since the 2.615 MeV radiation from ambient ^{208}Tl (ThC'') was unresolved from the 2.75 MeV radiation in the NaI spectra, it was necessary to take a background spectrum and subtract it from the data taken at each energy. The solid curve in part (a) of Figure 3 shows a combined spectrum and the dotted curve in part (a) shows a background spectrum. Part (b) shows the results of a subtraction of the two spectra and clearly shows the 2.75 MeV photopeak. A 50 cm^3

Figure 3. Line shapes observed for the $^{36}Ar(p,\gamma)^{37}K$ reaction with a 10.2 x 12.5 cm NaI crystal. The solid line in part a) shows the combined radiations from ^{37}K and the ^{208}Tl which was present as a background contaminant. The dotted curve shows the background radiation with no beam. Part b) depicts the the subtraction of the background from the original data, and represents the capture γ-ray photopeak.

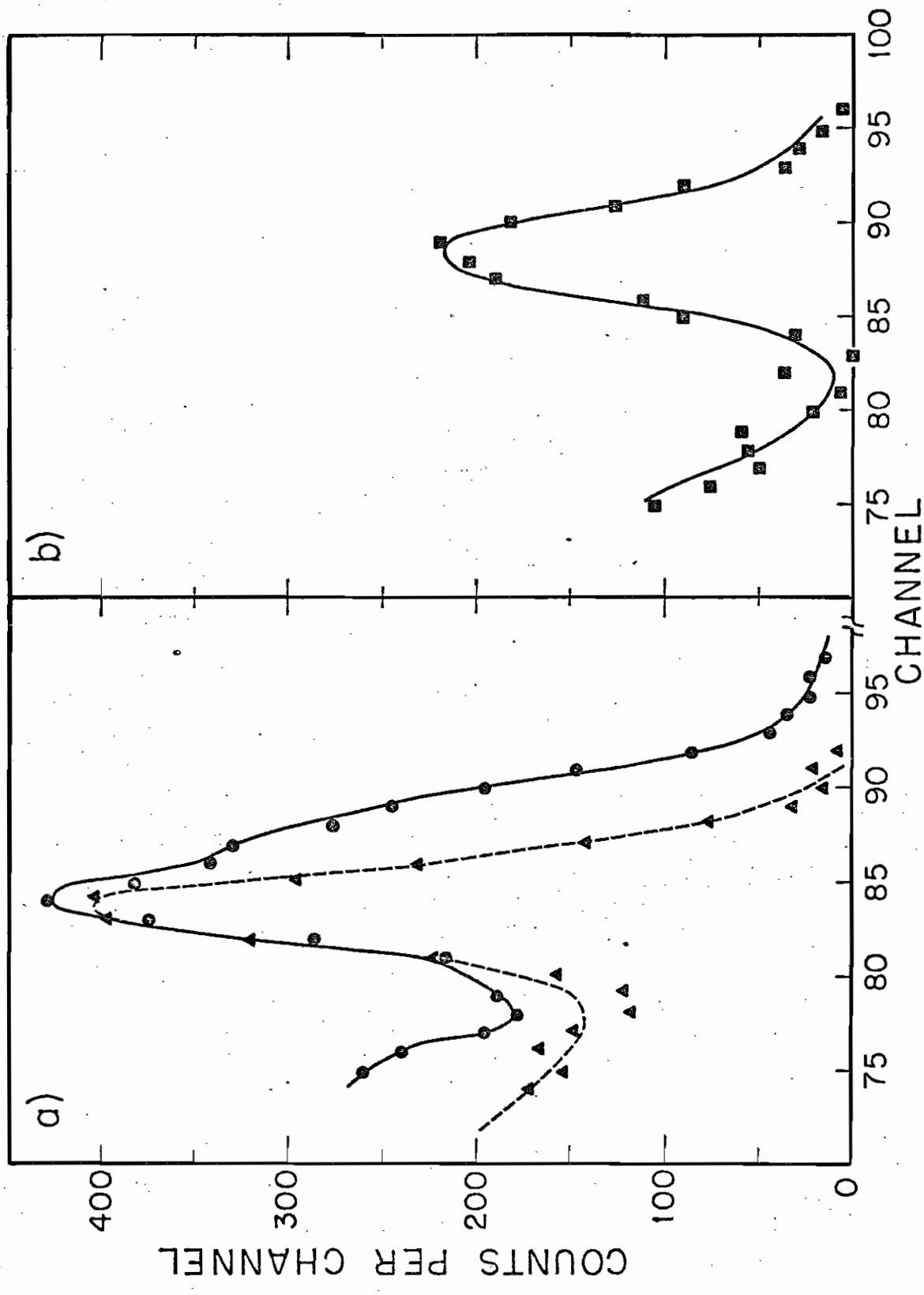
a)
b)
COUNTS PER CHANNEL
CHANNEL
0
100
200
300
400
75
80
85
90
95
100

Figure 4. Gamma ray yields from the $^{36}Ar(p,\gamma)^{37}K$ reaction versus proton energy with the ion implanted foil as a target. The capture resonance at 0.918 MeV has a width of 0.8 keV and thus can be used to measure the distribution of argon in the foil. The solid curve shows the relative distribution of ^{36}Ar in the tantalum substrate.

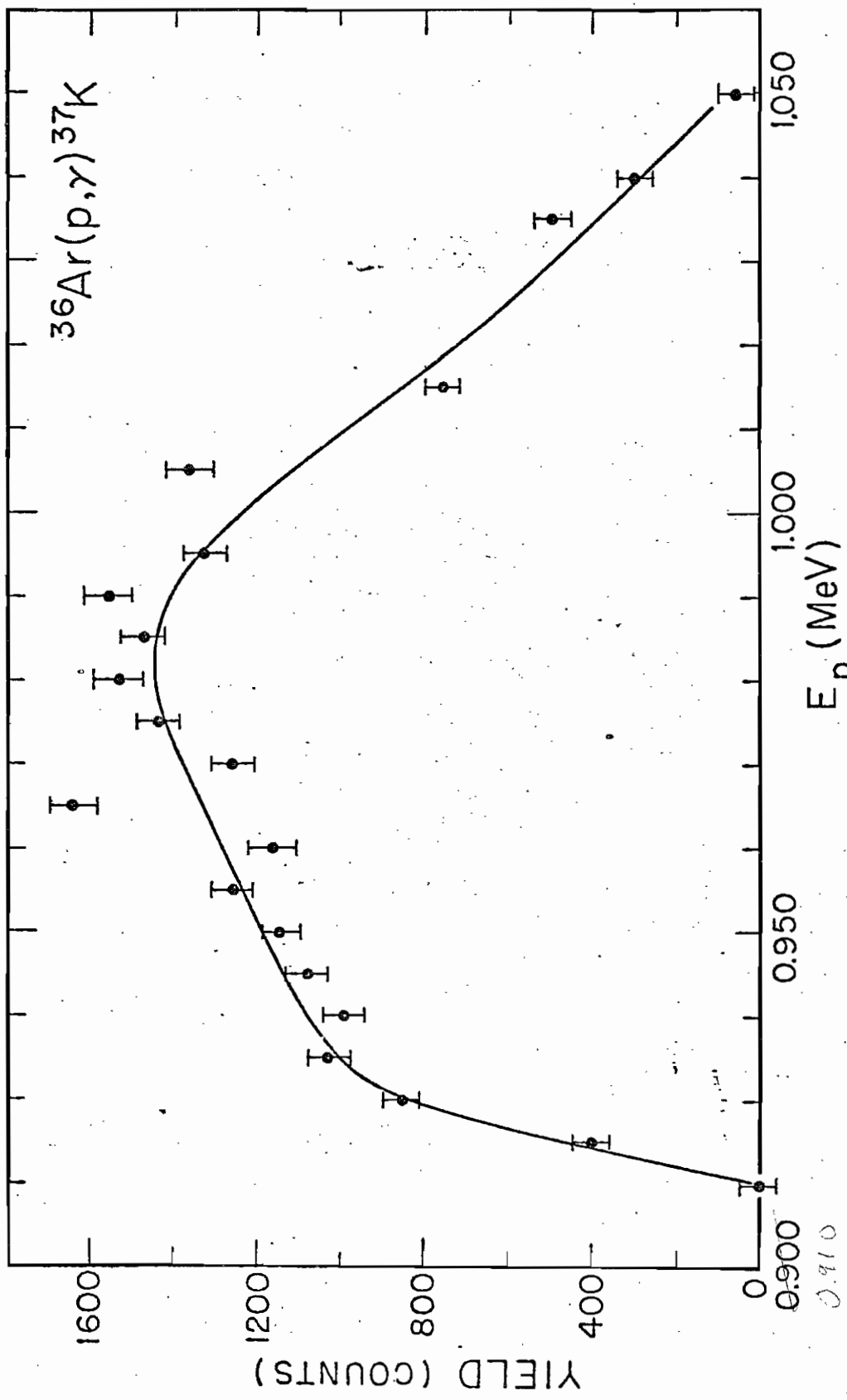
$^{36}Ar(p,\gamma)^{37}K$
YIELD (COUNTS)
0
400
800
1200
1600
0.900
0.950
1.000
1.050
E_p (MeV)

Ge(Li) γ-ray detector was used to assure that the unresolved components in the NaI spectra were indeed from ^{37}K and ^{208}Tl. At maximum yield the count rate in the photopeak of the Ge(Li) detector was about 1 count per minute and the count rate in the photopeak of the combined $^{37}K/^{208}Tl$ spectra was about 66 counts per minute. The count rate due to ^{208}Tl alone was 30 counts per minute. Figure 4 shows the yield curve obtained from the NaI data.

E. Reaction Product Detection

1.Gamma-ray Detection

During the course of this study three different Ge(Li) detectors were used with active volumes of 30, 50 and 80 cm^3, and with resolutions (measured at 1.332 MeV) of 2.8,2.2 and 4 keV respectively. The large volume detector had higher efficiency for detection of γ-rays but the time resolution possible with its pulses was appreciably poorer than with the two smaller detectors. The poorer time resolution had the effect of increasing the amount of background radiation appearing in the neutron coincident γ-ray spectra.

2. Neutron Detection

The neutrons were detected with a 10.2 x 12.7 cm NE213 liquid scintillator mounted on a XP1040 phototube. The NE213 liquid is sensitive to both γ-rays and neutrons, but since the scintillations caused by neutrons decay slower than thoses caused by γ-rays, it is possible to distinguish between them. A circuit measuring the time difference between the leading edge of a pulse from the photomultiplier and the zero crossing of an amplified pulse was used to discriminate between γ-ray events

and neutron events. In order to lower the counting rate due to low energy γ and X radiation a 2.5 cm thick lead slab was interposed between the target and the scintillator. The arrangement for detectors is shown in Figure 1.

F.Data Acquisition

Figure 5 shows a block diagram of the four parameter data collection system which incorporates a pulser stabilizing system. The fast signals from the neutron and γ-ray detectors pass through discriminators and enter a time to amplitude converter (TAC). The amplitude of the linear output of the TAC is proportional to the time difference between the γ-ray signal and the neutron signal. This TAC also provides a logic pulse used to gate all linear signals, thus imposing an overall coincidence requirement on all information presented to the analog to digital converters (ADC's).

The output of the phototube is amplified and sent to an ADC and to a timing single channel analyzer (SCA) which serves as a zero crossing discriminator. The fast signal from the phototube passes through a leading edge discriminator. The time difference between the outputs of the discriminator and the SCA is determined by the decay constants of the scintillations, which are a function of whether they were caused by γ-rays or neutrons. A second TAC measures this time difference (PSD) and the linear TAC output is digitized by an ADC. The amplified linear signal from the γ-ray detector is checked for pileup before being processed by an ADC.

To insure that the gain and zero intercept of the γ-ray amplifier

Figure 5. A block diagram of the electronic setup for the four parameter data collection system with pulser stabilization. Abbreviations used are:

TAC = time to amplitude converter

BLR/PILEUP = baseline restorer and pileup rejector

ADC = analog to digital converter

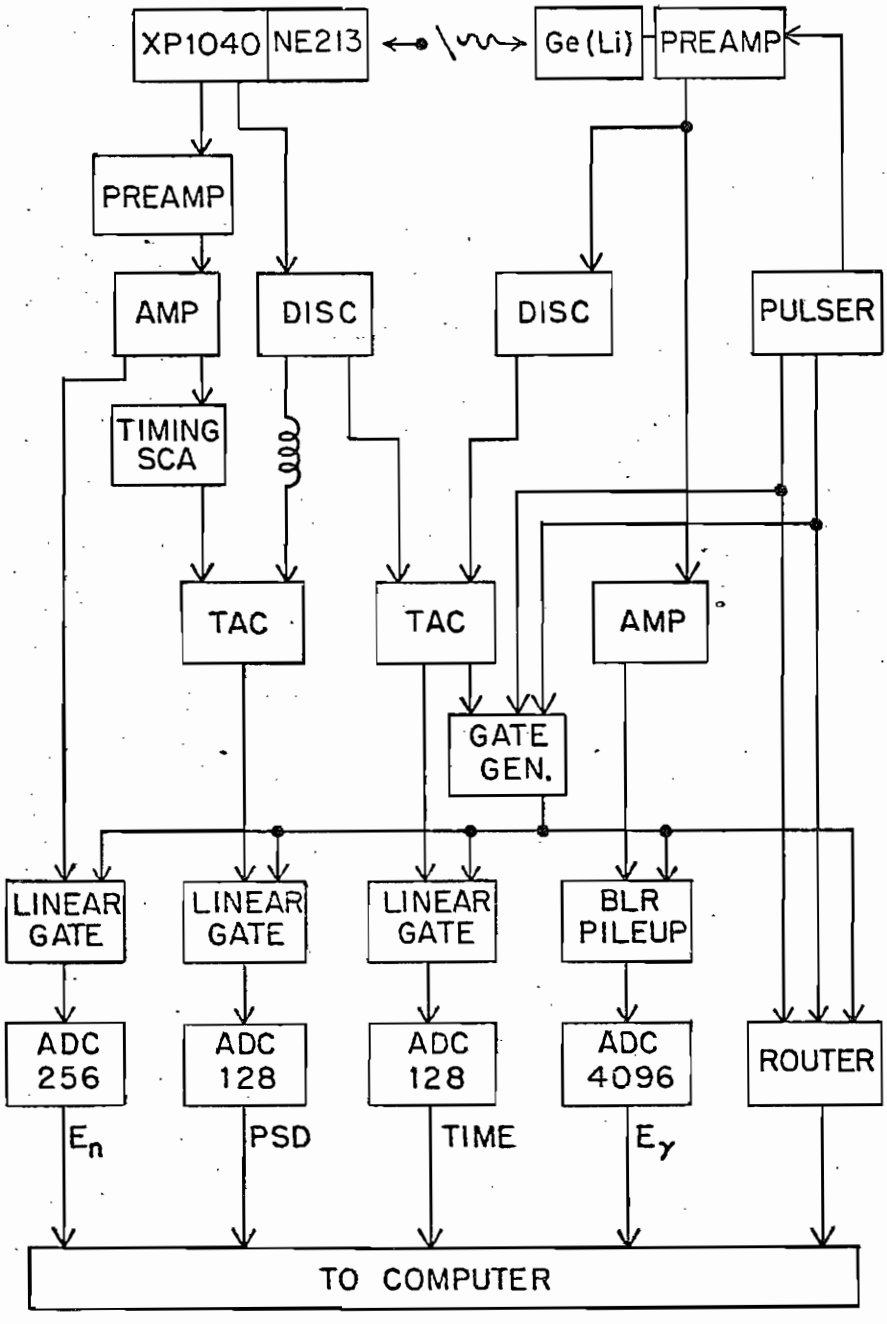
XP1040
NE213
Ge(Li)
PREAMP
PREAMP
AMP
DISC
DISC
PULSER
TIMING SCA
TAC
TAC
AMP
GATE GEN.
LINEAR GATE
LINEAR GATE
LINEAR GATE
BLR PILEUP
ADC 256
ADC 128
ADC 128
ADC 4096
ROUTER
E_n
PSD
TIME
E_γ
TO COMPUTER

and ADC system remained constant throughout an experiment, a precision double pulser was added to the γ-ray side of the electronics. The alternately large and small amplitude pulses from the pulser were sent to the input of the preamplifier, and at the same time a logic pulse was sent to the computer to identify the amplified Ge(Li) signal as a calibration pulse. The amplitudes of the pulses were set so that they corresponded to the upper and lower ends of the γ-ray spectrum. The stability of the pulser was checked over a three day period and the gain was found to drift less than one part in 10^4.

For each coincidence event, four binary numbers were stored in a buffer: E_γ, E_n, PSD and TIME. After 150 events (∿2 minutes) the data was recorded on magnetic tape for later analysis. After the pulser was added to the experimental apparatus, the running centroids were stored as the last two words in the buffer. The data could be observed on an oscilloscope as it accumulated to assure that the entire circuit was operating satisfactorily.

Chapter III

EXPERIMENTAL PROCEDURE

After focusing the beam onto the target, the beam current was adjusted so that the count rate in the Ge(Li) detector was as high as possible without degrading the resolution of the detector. Above $\sim 10^4$ counts per second the resolution was unacceptable. If γ-rays were to be measured at angles smaller than 50° , the liquid scintillator had to be positioned at distances greater than 150 cm from the target. During the first runs with θ_γ near 90° the scintillator was positioned at 75 cm from the target to maximize the counting rate. From these data the principal γ-ray decay modes were determined. Later data was taken with the scintillator at a distance of 150 cm, which allowed both positive and negative Doppler shifts to be measured.

The procedure followed during a typical run was to position the γ-ray detector at an angle and determine the gain of the Ge(Li) detector system with a ^{56}Co source. As this source emits many strong γ-rays from 0.846 to 3.253 MeV of accurately determined intensity and energy (Camp 1971) the spectra obtained can also be used to measure the relative efficiency of the detector as a function of energy. The source used in this experiment was made by bombarding an iron disk with a proton beam, creating the ^{56}Co through the (p,n) reaction. After completion of the calibration, the beam was put on the target, and data was collected at the chosen angle for about 12 hours. The beam was then removed from the target area, and another calibration spectrum taken before disturbing the

γ-ray detector. During a run several sets of data were taken at the chosen angles.

Both targets were positioned accurately so that the axis of rotation of the Ge(Li) detector passed through them. The Ge(Li) detector was put in place on the rotating table so that its axis was normal to the axis of radiation and passed through the center of the target. The liquid scintillator was always positioned at 0° with respect to the beam axis.

The buffered data were analyzed at a later time with the TUNL off-line computer. In order to obtain neutron associated γ-ray spectra with the least amount of background only those events associated with neutron events in both the PSD and TIME spectra were retrieved from the buffered tapes. To impose this criterion on the γ-ray events being retrieved from the tape, a two dimensional spectrum of PSD versus E_n was read from the magnetic tape. The neutron region was encircled with a light pen, setting a table of numbers in the analysis program. Then a time spectrum was read from the same run with only those TIME events associated with the table of PSD versus E_n numbers (PSD,E_n) being transferred to the data block in the analysis program. The channel numbers for the time coincidence peak and an equally wide random coincidence window were entered into the program. The γ-ray spectrum was then read from the data tape with only those γ-ray events associated with the [PSD,E_n,TIME(true,random)] numbers being stored. The γ-ray numbers associated with random time events were entered as negative numbers, thus subtracting "random" coincidences from the "true" coincidences. A typical spectrum obtained in this manner is shown in Figure 6. Part (a) shows the γ-rays detected in coincidence with neutrons detected in the NE213 scintillator, while part (b) shows the γ-rays in coincidence with other γ-rays detected in

Figure 6. Two typical Ge(Li) energy spectra taken with the 80 cm^3 detector. The data, taken at $\theta_\gamma = 90°$, are from the same run. The spectrum in part (a) is the result of applying the neutron coincidence criteria as outlined in Section F, Chapter II, while the spectrum in part (b) shows those γ-ray events that were in coincidence with γ-like scintillations in the neutron detector. The 0.511 MeV photopeak from annihilation radiation is truncated.

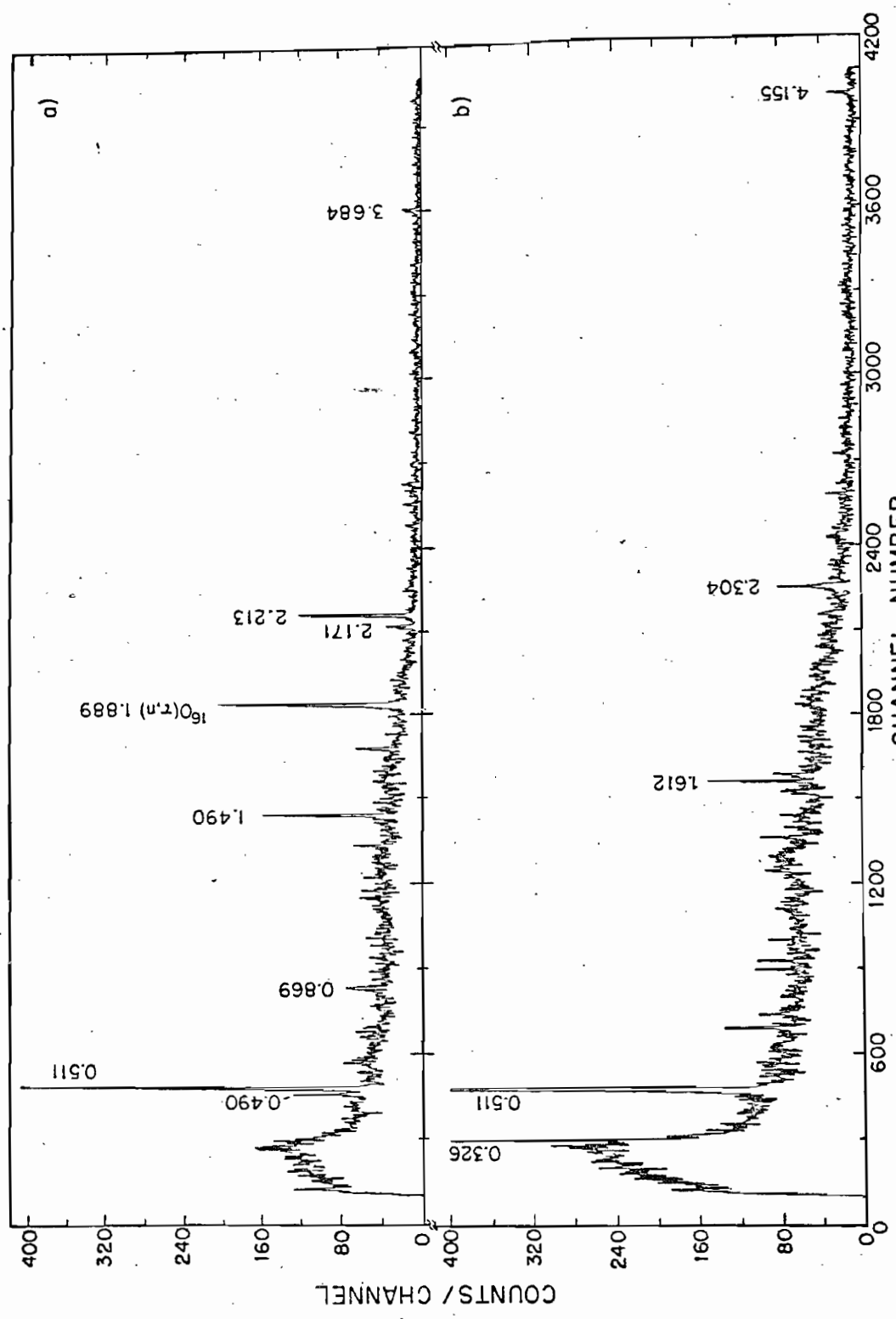
a)
b)
0.511
0.490
0.869
1.490
16O(τ,n) 1.889
2.171
2.213
3.684
0.326
0.511
1612
2.304
4.155
COUNTS / CHANNEL
CHANNEL NUMBER
0
80
160
240
320
400
600
1200
1800
2400
3000
3600
4200

the NE213 liquid scintillator.

Each record on the magnetic tape held 300 words (149 two-word events plus the two running centroids). The γ-ray spectra were stabilized with these centroids during the read back procedure. The analysis program used the first set of centroids to calculate the slope and the intercept of the gain, and then matched subsequent records to this initial one. To avoid having holes in the shifted spectra, a fraction of a channel was added to each stabilized record in a cyclic manner. For instance, if 0.4 was added to the nth record, then 0.5 would be added to the (n+1)th record and -0.5 to the (n+2)th record. Since the channel numbers are integers, this has the effect of randomizing where a break in the spectra will occur. Since the data is by nature random, it is not necessary to use a random number generator to randomize the adding of these numbers to the data.

Centroids of the photopeak in the neutron associated γ-ray spectra were obtained from first moment calculations after first subtracting a fitted quadratic background from the spectra in the region of the peaks of interest. The energies corresponding to the centroids were calculated using the calibration spectra taken before and after the run. The energy was calculated using the known energy of the two closest reference peaks below and above the peak of interest. To determine an experimental attenuation factor the experimental shifts and the maximum possible shifts must be known.

The maximum shifts were calculated from the reaction kinematics taking the size of the neutron detector into account and in the case of the gas cell correcting for the energy loss of the ^{3}He beam in the entrance foil. It was assumed in these calculations that the yield of the reaction

was proportional to the energy of the ^{3}He above threshold. The measured spatial distribution of ^{36}Ar in the tantalum foil was used in the calculations of the average recoil velocities. A linear least squares fit to the photopeak energies versus $\cos(\theta_{\gamma})$ determined $F(\tau)$. Theoretical attenuation factors were calculated for each level using the recoil velocities calculated by the kinematics program. The electronic stopping power coefficient, k_e, was set to 1.0 for the case of ^{38}Ca stopping in the tantalum foil, and to 1.0 for stopping in the gas. These values correspond to experimental measurements by Fastrup et. al.(1966) for ions stopping in solids, and Donahue et. al.(1971) for gaseous stoppers.

Chapter IV

EXPERIMENTAL RESULTS

A. Method of Analysis

This study has provided the precise energies for the six excited states of ^{38}Ca below 4.4 MeV and has resolved a suspected doublet at 3.7 MeV. Mean lifetimes for five of the six excited states has been determined with the Doppler shift attenuation method. The previous information about the levels is summarized by Paddock(1972). Levels at 0.0, 2.206, 3.695, 4.191, and 4.381 MeV with quoted errors of ±5 keV were observed by Paddock with the $^{40}Ca(p,t)^{38}Ca$ reaction and the measured angular distributions were fitted with L = 0,2,3 and 2 for the ground, 2.2, 3.7 and 4.4 MeV states, respectively. The work of Davies, et.al., also with the (p,t) reaction, confirms these findings. The work of Shapiro,et.al. with the $^{36}Ar(^{3}He,n)^{38}Ca$ reaction at 9 and 10 MeV is essentially in agreement with these findings except that the angular distributions of the neutrons associated with the level observed at 3.69 MeV was best fitted by distorted wave Born Approximation calculations with L = 2.

The shapes of the angular distributions in the above experiments are characteristic of the L transfer. With the zero spin targets, the final angular momentum of the product nucleus is equal to the total angular momentum transferred. Since the neutrons bound in the triton (and the protons in the ^{3}He) are in a spatially symmetric state (i.e. the transferred spin is zero) the final spin is equal to the L transfer.

The selection rule for the parity change is $\Delta\pi = (-1)^L$. Therefore, the spins and parities are determined for those states with a measured L-value. It should be noted that for the level at 3.7 MeV the different L-value assignments from the (p,t) and (^{3}He,n) experiments, 3^- and 2^+ respectively, suggest a possible doublet with spins and parities of 3^- and 2^+.

The levels and excitation energies as determined in this experiment are shown in Figure 7. The spins and parities are taken from the ℓ-value assignments as discussed above. Neutrons of a given energy deposit various amounts of energy as they collide with the atoms in the NE213 scintillator. Thus it is not possible to use the neutron energy spectra to accurately determine the energy of the various neutron groups. Thus the location of the various γ-ray transitions in ^{38}Ca had to be determined using the level energies from the reaction data. Fortunately these energies were accurate enough to allow unique placement of the transitions in the decay scheme. The fact that the ^{3}He bombarding energies of 9, 10, and 10.5 MeV used in this study were close to the 9.0 MeV bombarding energy used by Shapiro,et.al. also ruled out the population of any previously unobserved levels. Upper limits for branches other than those shown in Figure 7 are 15% except for the levels at 3.684 and 3.703 MeV where the limit is set at $\leq$6%.

Table 2 lists excitation energies with errors, the mean lifetimes and errors in these lifetimes as determined in this study. The errors listed for the mean lives include the statistical errors in the determination of the energies of the Doppler shifted γ-rays, the error due to feeding by gamma decay, and an error caused by an assumed uncertainty of 20% in the calculated stopping power.

Figure 7. Energy level diagram for ^{38}Ca depicting the observed γ-ray energies and transitions. The spin and parity assignments are from (Paddock 1972, Shapiro 1970). The doublet at 3.7 MeV was hitherto unresolved.

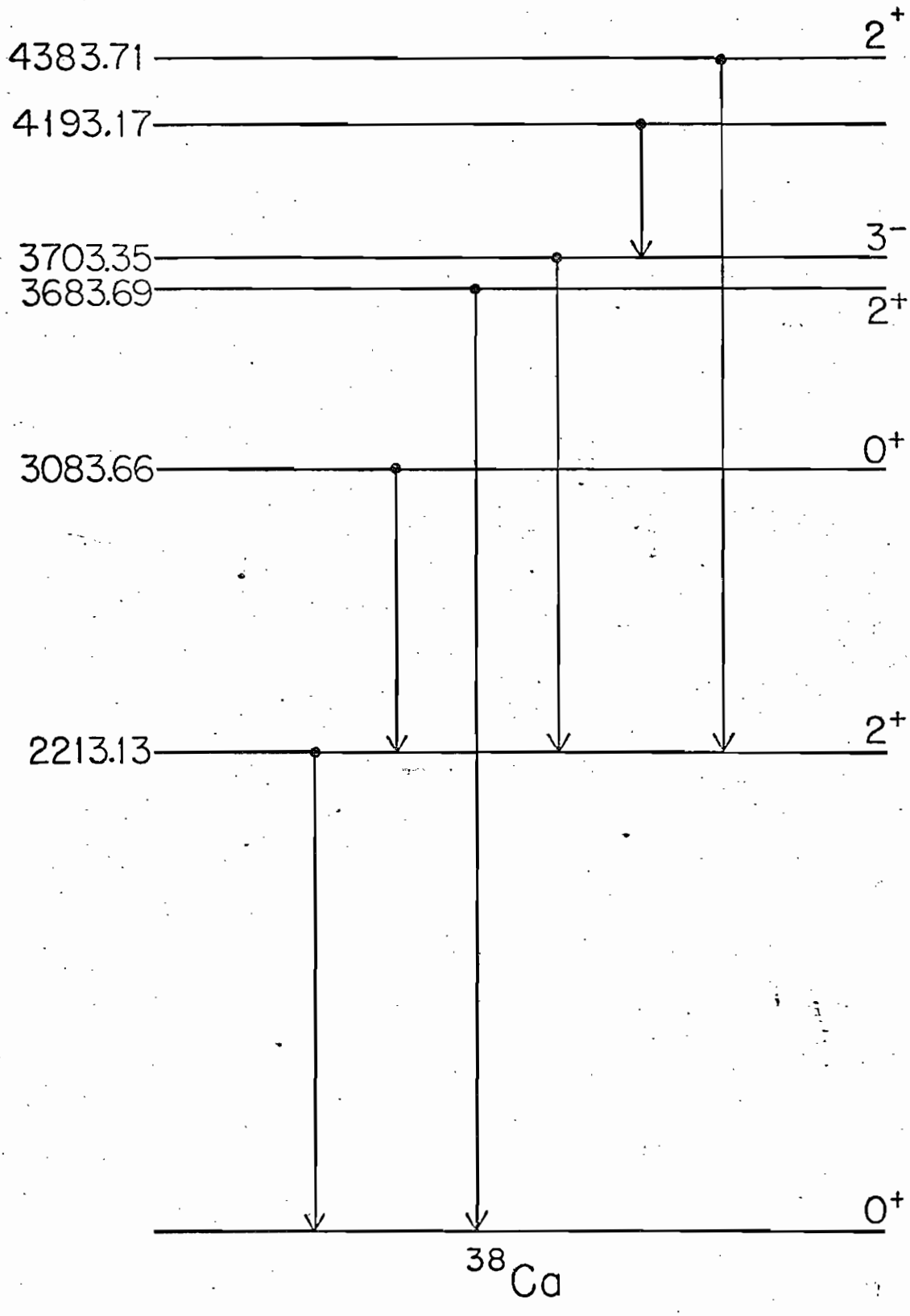
4383.71
2+
4193.17
3703.35
3-
3683.69
2+
3083.66
0+
2213.13
2+
0+
38Ca

Table II

Energies and Mean Lifetimes

of the First 6 Excited States

of ^{38}Ca

E_x	τ(fs)
2.21313±0.00010	$98\pm^{44}_{40}$
3.08366±0.00016	$27\pm^{14}_{10}\times10^3$
3.68369±0.00047	<8
3.70335±0.00015	$225\pm^{100}_{85}$
4.19317±0.00027	
4.38371±0.00045	$35\pm^{17}_{12}$

B. The Levels Above 2.3 MeV

1. The 4.384 MeV Level

The level observed by Davies, et.al. and Paddock, et.al. at 4.381± 0.005 and 4.391±0.020 MeV respectively was assigned a spin and parity of 2^+. The 2.17058±0.00044 MeV decay can be placed in the level scheme as a decay of this level at 4.3 MeV to the 2.21313 MeV $J^\pi = 2^+$ first excited state. Two typical spectra taken at 90° and 125° are shown in Figure 8. The measured Doppler shifts, when combined with the calculated maximum shifts yield an average experimental attenuation factor of 62.4±9.8%. This attenuation factor is based on 14 measurements during 3 different runs.

The multipolarity of a 2^+ to 2^+ transition can be mixed E2/M1. However, in most but not all cases, the M1 strength dominates the E2 strength. For the purpose of discussion the decay will be assumed to be pure M1.

In terms of Weisskopf units (Skorka 1966), a commonly used standard strength, the M1 transition strength of this decay is

$$|M|^2 = \Gamma/\Gamma_w = 0.09 \text{ W.u.}$$

This value is well within the range (Skorka 1966) of $10^{-3}<\Gamma<10$ W.u. which has been observed for $\Delta T = 0$, M1 transitions in nuclei with $A \leq 40$.

2. The Level At 4.191 MeV

The 0.490 MeV γ-ray shown in Figure 9 was observed at all bombarding energies and with both the solid and gaseous targets. To determine the source of this γ-ray within the level structure of ^{38}Ca, two different time windows were used to obtain γ-ray spectra from the buffered

Figure 8. Typical line shapes for the full energy peaks for the 4.384 → 2.213 MeV, $J^{\pi} = 2^{+} \rightarrow 2^{+}$ and 2.213 → 0.0, $J^{\pi} = 2^{+} \rightarrow 0^{+}$ transitions. The shifts shown are for the particular pair of runs. The $F(\tau)$'s shown are for the set of data taken with the 80 cm^3 Ge(Li) detector. See Table 2 for complete results.

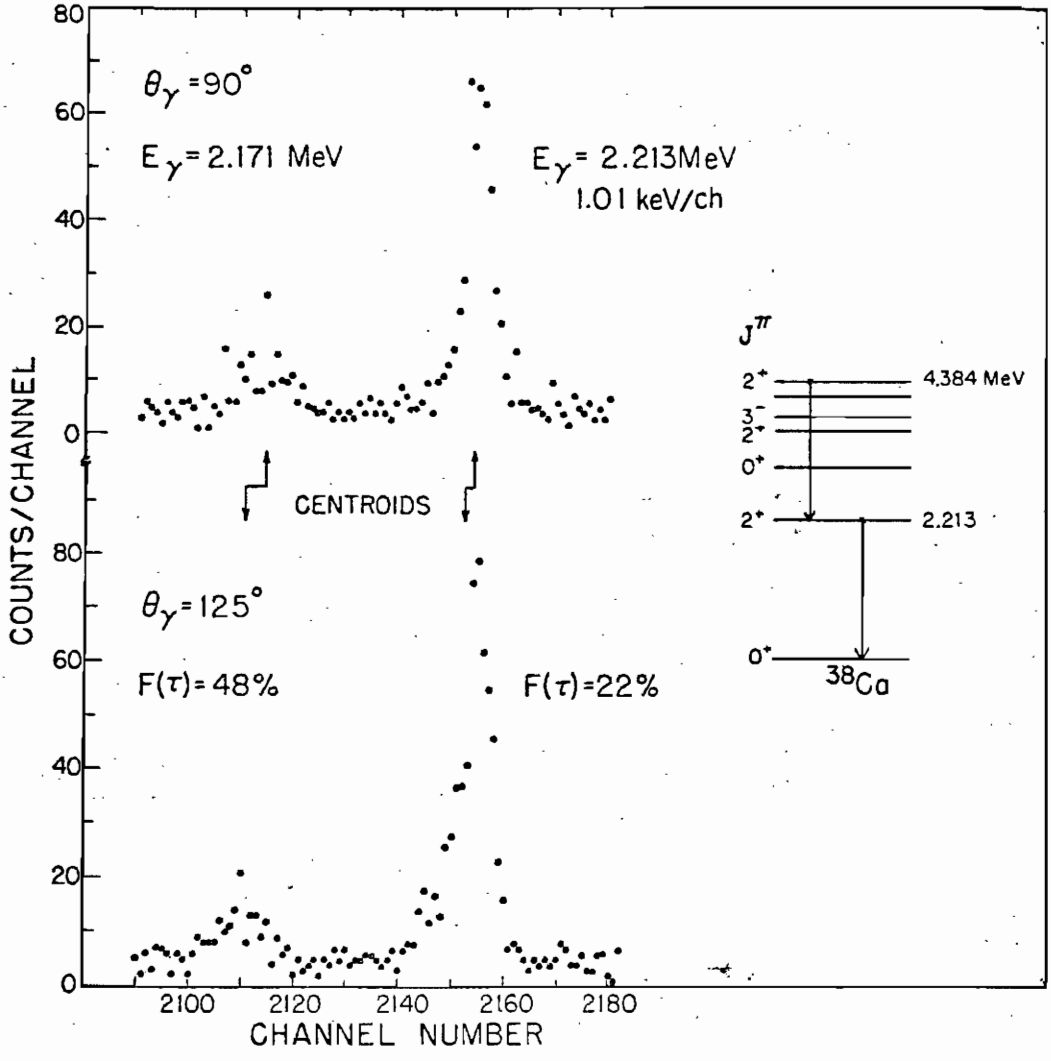
θγ=90°
Eγ=2.171 MeV
Eγ= 2.213MeV
1.01 keV/ch
CENTROIDS
θγ=125°
F(τ)=48%
F(τ)=22%
Jπ
2+
4.384 MeV
3−
2+
0+
2+
2.213
0+
38Ca
COUNTS/CHANNEL
CHANNEL NUMBER
0
20
40
60
80
2100
2120
2140
2160
2180

Figure 9. The 0.490 MeV photopeak from the 4.193 MeV to 3.703 MeV transition. Also shown is the 0.511 MeV photopeak from annihilation γ-rays.

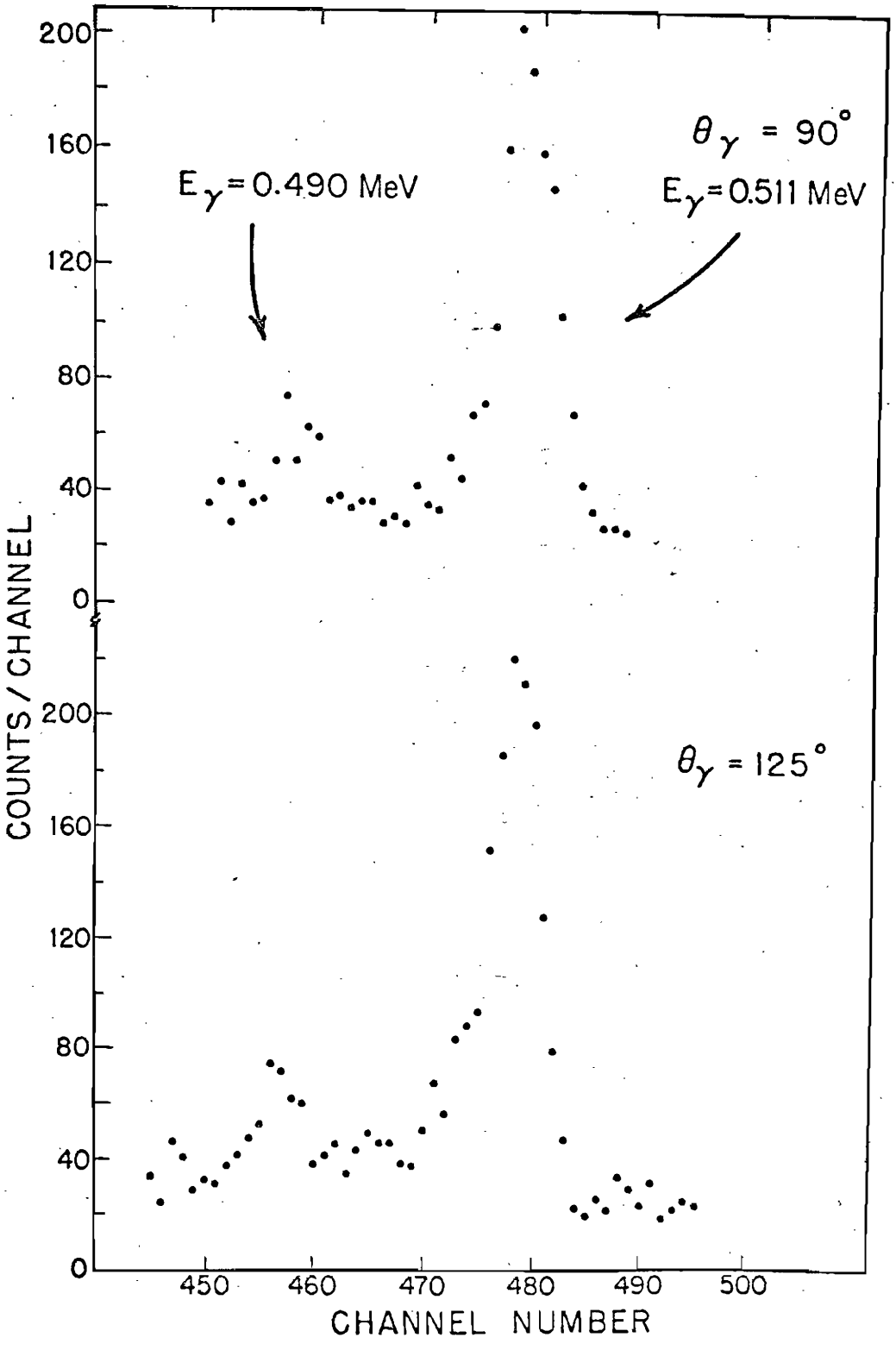
200
160
120
80
40
0
200
160
120
80
40
0
COUNTS / CHANNEL
E_γ = 0.490 MeV
θ_γ = 90°
E_γ = 0.511 MeV
θ_γ = 125°
450
460
470
480
490
500
CHANNEL NUMBER

data. The time spectrum of the neutrons from the $^{36}Ar(^{3}He,n)^{38}Ca$ reaction did not resolve individual neutron groups, but the ratio of faster to slower neutrons should be greater on the left-hand (lower time difference) side than on the right-hand side of the time spectra. Thus the time spectrum was divided into two parts, a "fast" half and a "slow" half. The 0.490 MeV radiation was only observed in γ-ray spectra obtained using the "slow" window. Since the neutrons from more highly excited states have lower energies than those from lower-lying levels, this decay originates from a state with large excitation energy. The level energies observed by Paddock (1971) include levels at 4.191 and 3.695 MeV. The energy of this decay fits the difference of the energies of these two levels and no others. On this basis, the the energy of this level is found to be 4.19317±0.00027 MeV.

Unfortunately, due to the large number of 511 keV γ-rays from annihilation radiation (the singles, i.e. non-coincident, count rate in the 511 keV full energy loss peak was on the order of 10^6 counts per hour) no reliable Doppler shifts could be extracted for this low yield γ-ray. Data from a typical pair of runs, one at 90° and one at 125° is shown in Figure 9 .

3. The Levels at 3.703 and 3.684 MeV

The two γ-rays with energies of 1.49022±0.00011 and 3.68369±0.00047 MeV resolve the suggested $J^{\pi} = 3^{-}, 2^{+}$ doublet at 3.7 MeV. Shapiro,et.al. (1970) have measured γ-rays in coincidence with neutrons from the $^{36}Ar(^{3}He,n)$ reaction. At a bombarding energy of 9 MeV, their NaI spectrum showed two γ-rays, one at 1.45 MeV and the other at 3.69 MeV. The higher γ-ray energy resolution of this experiment allows the assignment

of the 1.490 MeV γ-ray as a 3.703 → 2.213 MeV transition and the 3.683 MeV γ-ray as the ground state transition. The energies of these γ-rays yield level energies of 3.70335±0.00015 and 3.68369±0.00047 MeV, respectively.

The measured F(τ)'s are 99.6±9.0% (3.683 MeV) and 16.7±4.1% (3.703 MeV) and the associated lifetimes are <8 fs and 225^{+100}_{-85} fs, respectively. If the ground state transition were associated with the 3^- level, then the E3 strength would be greater than 10^6 W.u. This value is far beyond the range of observed E3 strengths (1-10 W.u.)(Endt 1974). Assuming pure transitions, alternate assignment of $J^\pi = 2^+$ for the 3.684 MeV level and $J^\pi = 3^-$ for the 3.703 MeV level yields an E2 strength of >22 W.u. and an E1 strength of 10^{-3} W.u. Both of these values are well within the range of strengths reported for this region of nuclei. Figures 10 and 11 show typical data from runs at $\theta_\gamma = 90°$ and 125°.

4. The Level at 3.084 MeV

A $J^\pi = 0^+$ level was observed at 3.06 MeV by Shapiro, et.al.(1969). This level was not seen in either the (p,t) studies of Davies, et.al. (1968) or Paddock (1971). The level observed by Shapiro decayed only to the first excited state with an 0.85 MeV γ-ray. The 0.87054±0.00047 MeV γ-ray observed in this study was assigned to the decay of this 0^+ level.

The decay γ-rays exhibited no Doppler shifts in any of the runs with the ion-implanted foil as target. A preliminary experiment was performed with isotopically enriched (99.6%) and chemically pure ^{36}Ar gas at 2 atmospheres pressure as target and stopping material. The F(τ) measured in this first experiment was 77±30%. In the next experiment the stopping power of the target was increased by raising the pressure

Figure 10. The 1.490 MeV γ-ray decay of the 3.703 MeV level is shown.

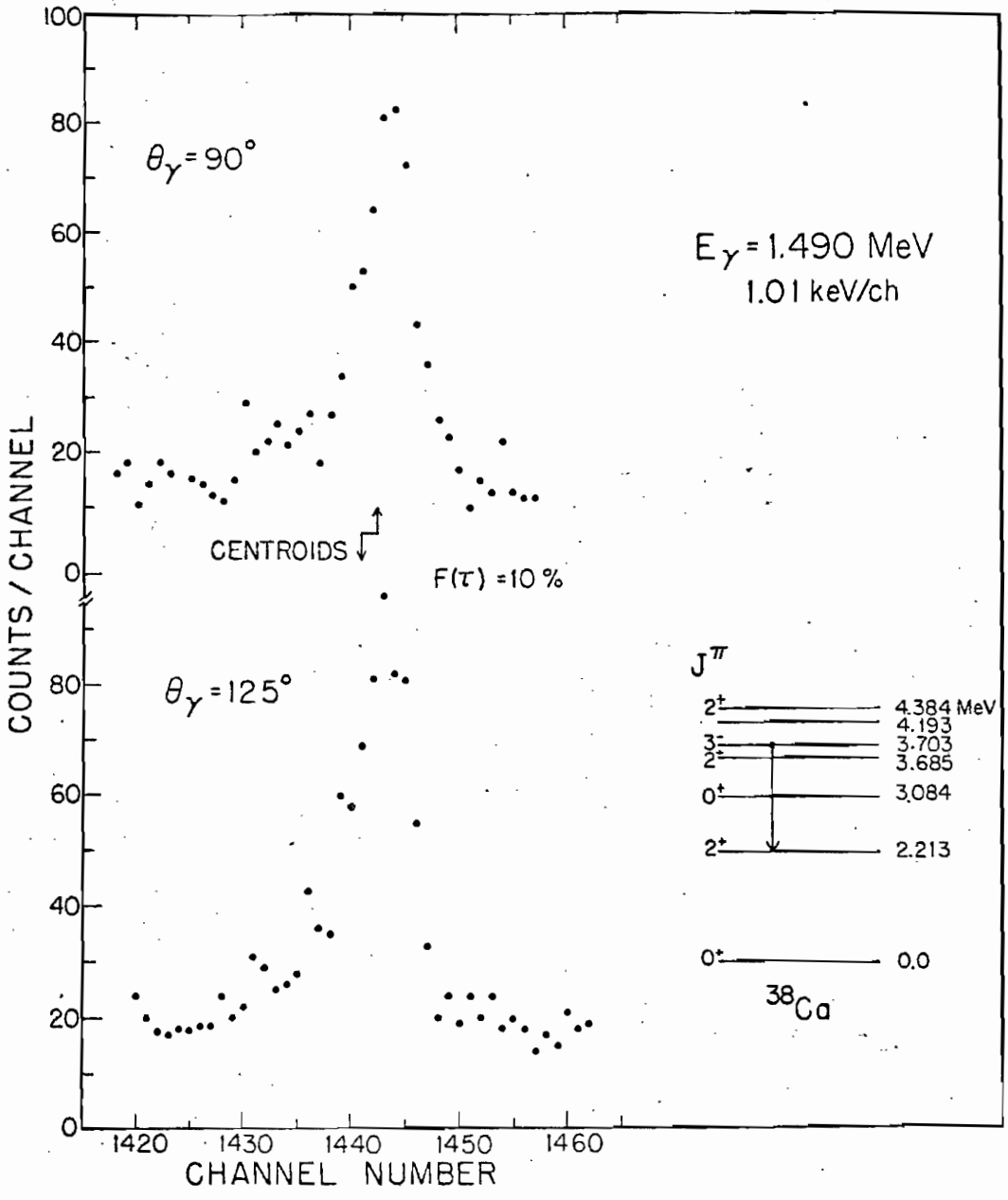
100
80
60
40
20
0
80
60
40
20
0
COUNTS / CHANNEL
θγ = 90°
θγ = 125°
CENTROIDS
F(τ) = 10 %
Eγ = 1.490 MeV
1.01 keV/ch
Jπ
2+ 4.384 MeV
4.193
3- 3.703
2+ 3.685
0+ 3.084
2+ 2.213
0+ 0.0
38Ca
1420
1430
1440
1450
1460
CHANNEL NUMBER

Figure 11. The full energy loss peak of the decay of the $J^{\pi} = 2^{+}$, 3.684 MeV level to the 0^{+} ground state. This peak and its associated double escape peak were fully shifted in all measurements.

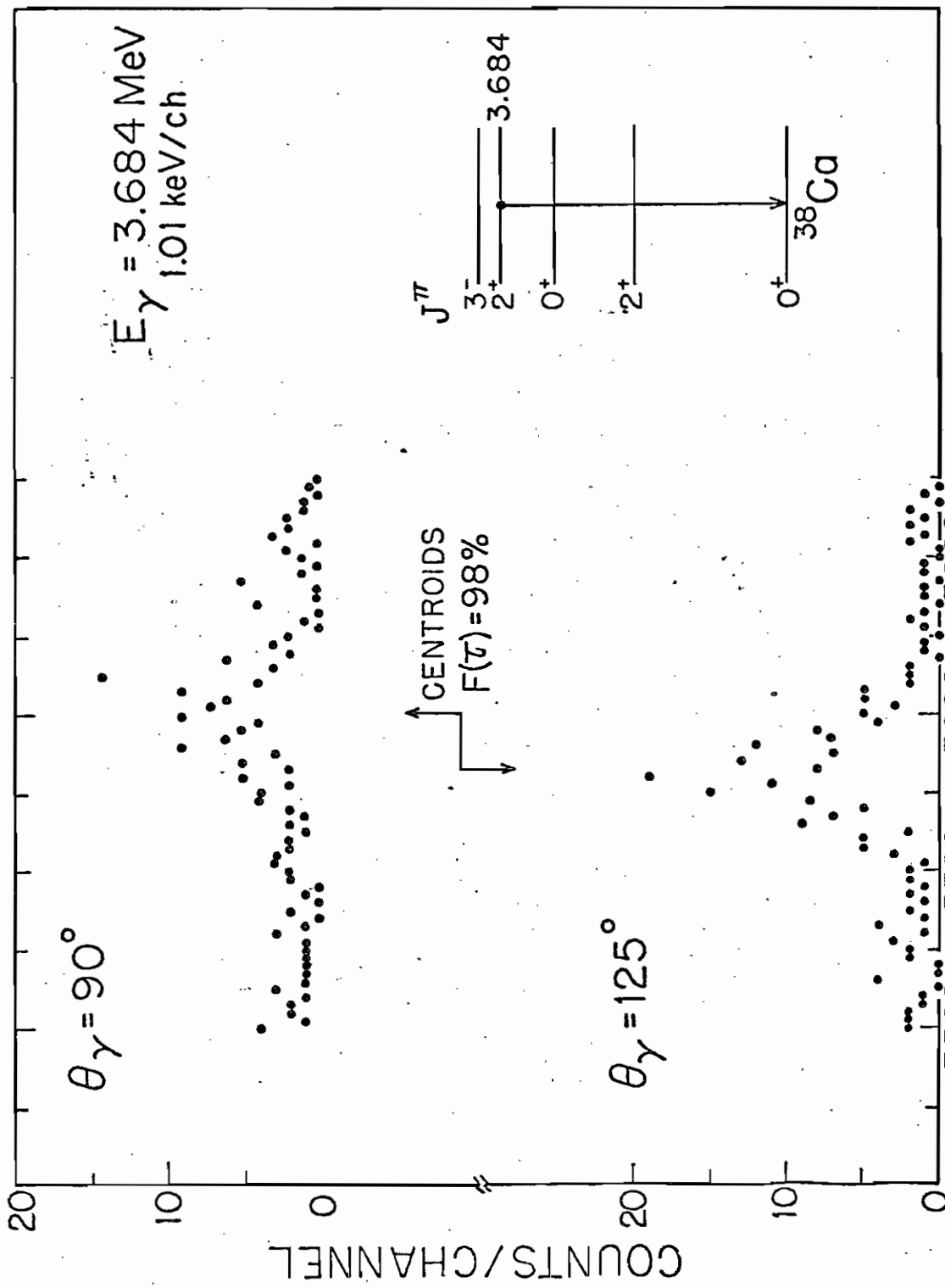
E_γ = 3.684 MeV
1.01 keV/ch
θ_γ = 90°
θ_γ = 125°
CENTROIDS
F(τ)=98%
J^π
3⁻
2⁺
0⁺
2⁺
0⁺
3.684
^{38}Ca
COUNTS/CHANNEL
CHANNEL NUMBER
20
10
0
20
10
0
3560
3580
3600
3620

to 6 atmospheres. Two $F(\tau)$ versus τ curves, one for ^{38}Ca recoiling in ^{36}Ar at 2 atm. and the other for ^{38}Ca recoiling in ^{36}Ar at 6 atm. shown in Figure 12 illustrate the effect of the pressure increase. The $F(\tau)$ resulting from the 6 atm. run was 73.8±8.2%. This value leads to a mean lifetime of $27\pm^{14}_{10}$ ps and an E2 transition strength of 8 W.u. The spectra shown in Figure 13 are from runs at $\theta_\gamma = 90°$ and $\theta_\gamma = 125°$ taken with the gas cell at 6 atm. using the 50 cm^3 Ge(Li) detector.

Figure 12. Theoretical attenuation factors versus τ for ^{38}Ca recoiling in ^{36}Ar gas at pressures of 2 and 6 atmospheres.

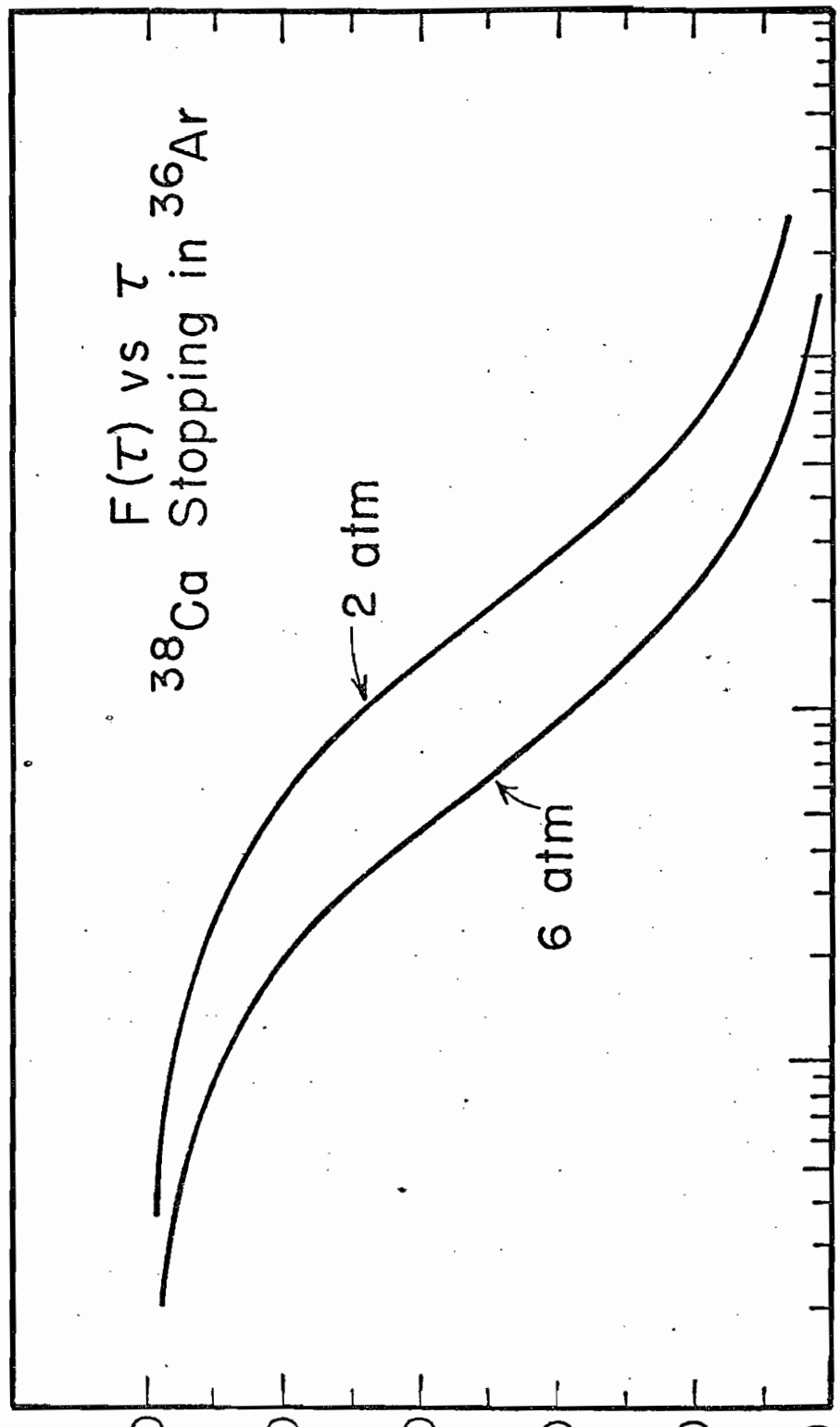
F(τ) vs τ
38Ca Stopping in 36Ar
2 atm
6 atm
F(τ) (%)
100
80
60
40
20
0
1
10
100
1000
τ (ps)

Figure 13. The full energy peaks for the 0.869 MeV transition between the 3.073 MeV level and the 2.213 MeV level. This peak did not exhibit a Doppler shift with the ion-implanted target. The data shown was taken with the gas cell.

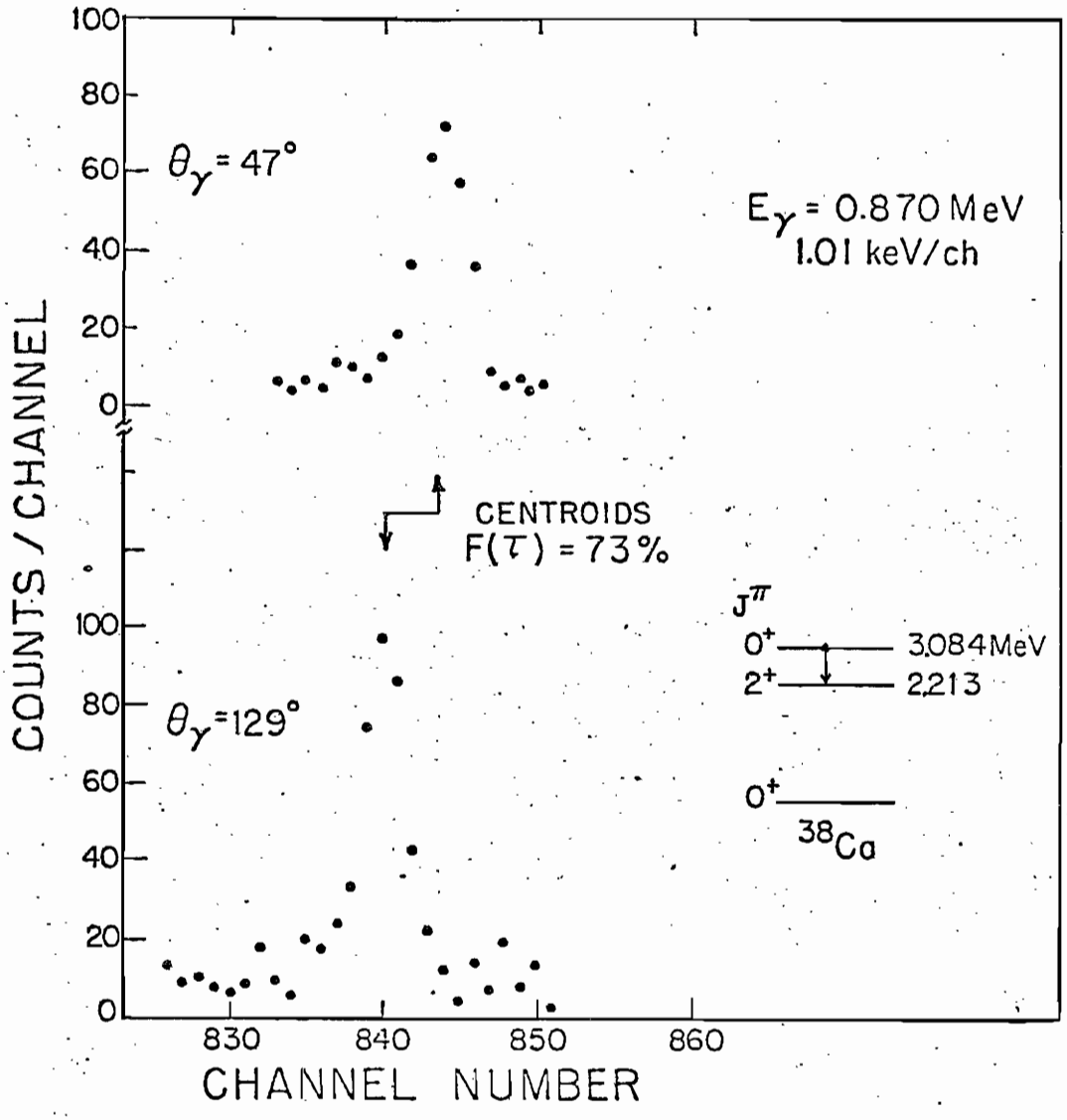
100
80
60
40
20
0
$\theta_\gamma = 47°$
$E_\gamma = 0.870$ MeV
1.01 keV/ch
CENTROIDS
$F(\tau) = 73\%$
J^π
0^+ 3.084MeV
2^+ 2.213
0^+
^{38}Ca
100
80
60
40
20
0
$\theta_\gamma = 129°$
COUNTS / CHANNEL
830
840
850
860
CHANNEL NUMBER

C. The 2.213 MeV Level

The $J^{\pi} = 2^{+}$, 2.313 MeV first excited state of ^{38}Ca is fed by gamma transitions from the 3.084, 3.703 and 4.383 MeV levels. The relative proportions of feeding and direct populations were determined from γ-ray data acquired at an angle $\theta_{\gamma} = 125°$. Since the $P_2(\cos\theta)$ term of the expansion of the angular distribution is zero at 125° and the $P_2(\cos\theta)$ is small, photopeak areas measured at this angle are proportional to the direct populations. The direct and indirect populations of the 2.213 MeV level from the reaction and from the feeding by the 3.084, 3.703 and 4.384 MeV levels was found to be 0.23±0.07, 0.06±0.01, 0.50± 0.04 and 0.21±0.03, respectively. In this case, the lifetime must be obtained from the equation (see Appendix A)

$$F_{obs} = \nu_0 F_0(\tau_0) + \sum \nu_i \frac{\tau_i F_i(\tau_i) - \tau_0 F_i(\tau_0)}{\tau_i - \tau_0}$$

where F_{obs} is the observed attenuation factor for a state of lifetime τ_0 with a direct population ν_0 and indirect population ν_i from states with mean lifetimes τ_i and where $F_n(\tau)$ is the attenuation factor for a lifetime τ and an initial recoil velocity equal to that of state n. From the experimentally measured ν's and τ's, the lower curve shown in Figure 14 was obtained. Also shown in Figure 14 is the $F(\tau)$ curve (upper) that would be used if there were no feeding by gamma decays. A typical set of photopeaks for this decay are shown in Figure 8. The average attenuation factor from the experiments with the implanted foil as a target is 14.2±2.3% and yields a lifetime of $98 \pm \frac{44}{40}$ fs and an E2 trans-

ition strength of $20.5 \pm^{8}_{9.4}{}^{.6}$ W.u.

Figure 14 . $F(\tau)$ versus τ curves for ^{36}Ar recoiling in the ion-implanted tantalum foil. The upper curve is for a directly populated state of E_x = 2.213 MeV. The lower curve is for the 2.213 MeV state with 0.23 direct population and proportions of population by gamma transitions of 0.06, 0.50 and 0.21 from the levels at 3.084, 3.703 and 4.384 MeV.

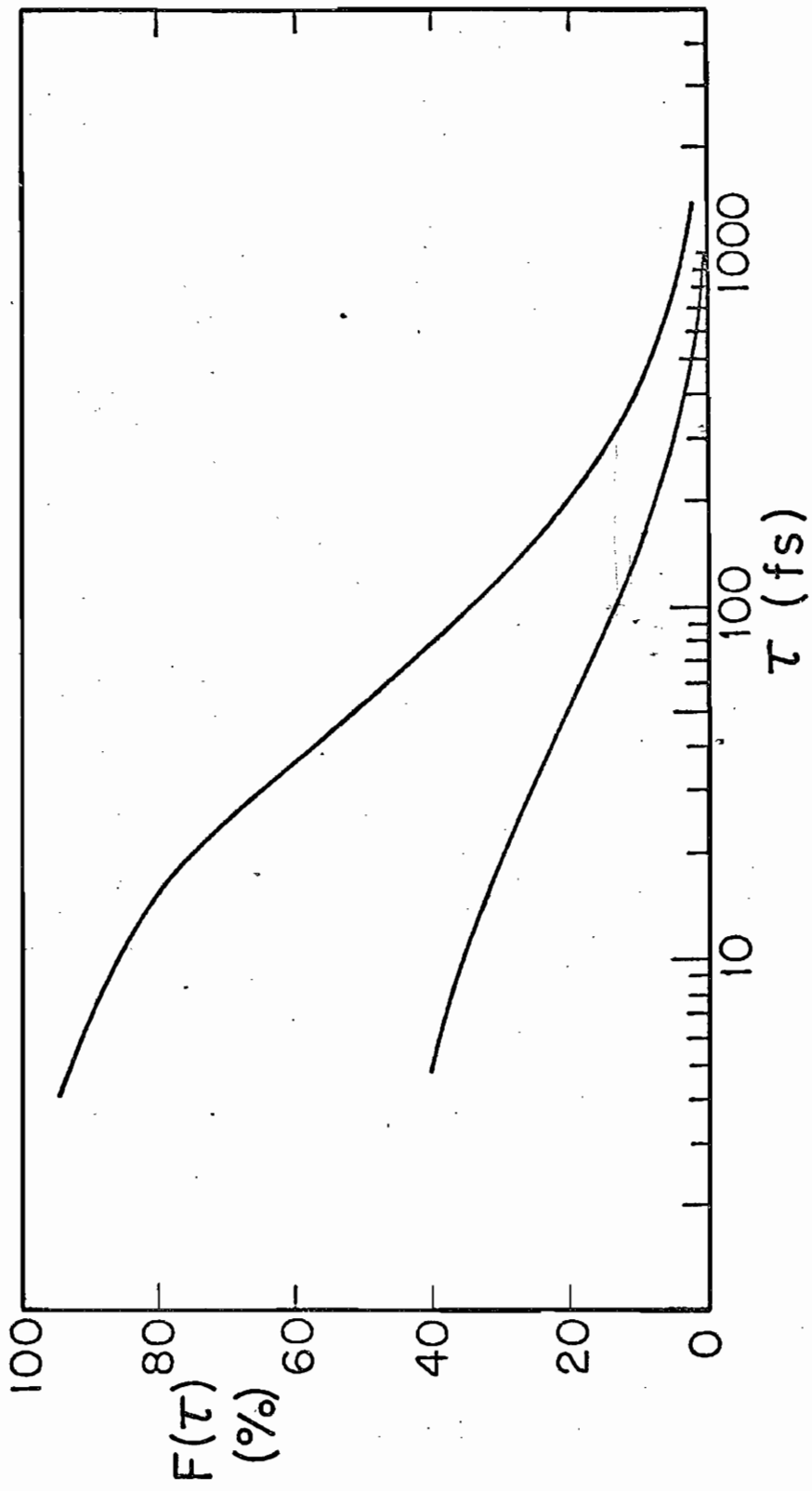
100
80
60
40
20
0
F(τ)
(%)
10
100
1000
τ (fs)

Chapter V

DISCUSSION

The three A = 38 nuclei, ^{38}Ar, ^{38}K and ^{38}Ca are members of an isobaric triplet, and it is of interest to compare the transition strengths of similar transitions in the three nuclei. The level structure and strengths determined in this study of ^{38}Ca permit such a comparison for the first time. Figure 15. shows the levels below 3 MeV for these nuclei. The $J^{\pi} = 2^{+}$, T = 1 level at 2.4 MeV in ^{38}K decays to the T = 1, 0^{+} level at 0.130 MeV with a 6% branch. The lifetime shown is the average of measurements by Hasper *et. al.*(1973) and by Engmann *et. al.*(1971). The lifetime for the corresponding $2^{+} \rightarrow 0^{+}$ transition shown for ^{38}Ar is from the study of Engelbertink *et. al.*(1969).

The width of a transition, $\Gamma(L)$, is related to the transition strength B(L) by the relation of Alder *et. al.* (1956)

$$\Gamma(L) = \frac{8\pi(L+1)}{L[(2L+1)!!]^2}\left[\frac{E}{\hbar c}\right]^{2L+1} B(L)$$

where the total width $\Gamma_{total} = \frac{\hbar}{\tau} = \sum \Gamma(L)$. Following the work of Warburton *et. al.*(1969) the transition matrix element can be divided into two parts, one independant of T_3 and one linearly dependant on T_3. For a transition with no change in T, the matrix element becomes

$$M.E. = (2T+1)^{-1/2}\delta_{T_iT_f}\langle J_fT_f|H_{IS}|J_iT_i\rangle + \frac{T_3}{[T_i(T_i+1)(2T_i+1)]^{1/2}}\langle J_fT_f|H_{IV}|J_iT_i\rangle$$

Figure 15. The low-lying levels of the A = 38 isobaric triplet. The lifetimes, spins and parities for ^{38}Ar are from (Engelbertink 1969) and those for ^{38}K are from (Hasper 1973, Engmann 1971).

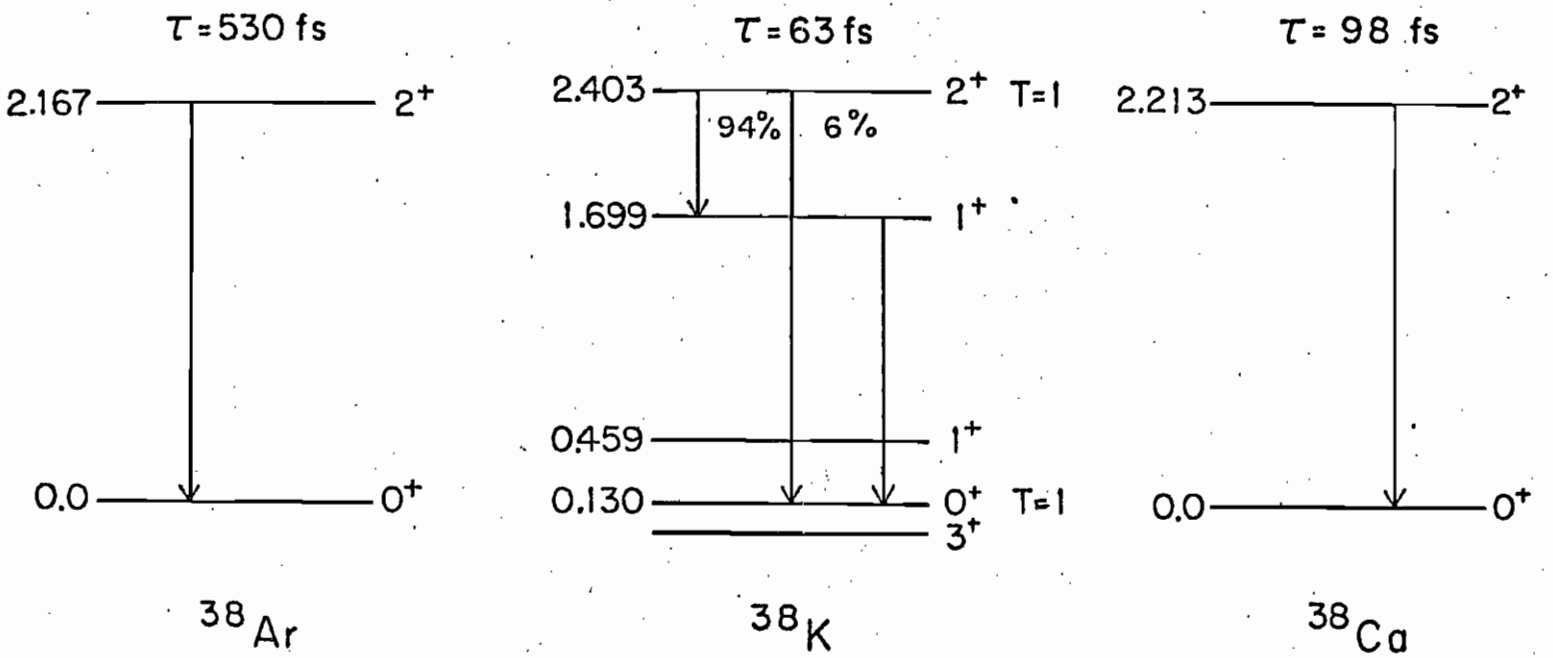
τ = 530 fs
2.167
2+
0.0
0+
38Ar
τ = 63 fs
2.403
2+ T=1
94%
6%
1.699
1+
0.459
1+
0.130
0+ T=1
3+
38K
τ = 98 fs
2.213
2+
0.0
0+
38Ca

For a pure E2 transition, with $\Delta T = 0$,

$$\Gamma = K[\, a + \frac{T_3 b}{\sqrt{2}}]^2$$

where

$$K = 8\pi(E_\gamma/\hbar c)^5(3/1350)$$

and

$$a = \langle J_f T_f | H_{IS} | J_i T_i \rangle$$

and

$$b = \langle J_f T_f | H_{IV} | J_i T_i \rangle .$$

Thus a measurement of the widths of an analogous transition in all three members of an isobaric triad can determine a and b. For the case of the A = 38 triad a least squares fit to the data gives values $a^2 = 4.2 \times 10^{-2}\ e^2f^4$ and $b^2 = 1.2 \times 10^{-2}\ e^2f^4$. Since the form of the matrix element remains the same when it is written in terms of effective charges, e_p and e_n (Glaudemans et. al. 1971), i.e.

$$\Gamma(E2) = K[\delta_{T_f T_i}(e_p+e_n)a - \langle T_i T_{3i} 10 | T_f T_{3f}\rangle (e_p-e_n)b]^2$$

the ratio, α, of the isovector to isoscalar components determines the value of the ratio of the difference of the effective charges to their sum. As the square root of the width is linear in T_3 the data shown in Figure 16 for the isobaric triplets of masses 30, 34 and 38 are plotted as $\Gamma^{1/2}$ versus T_3. The value of α for each case is also shown. No other isobaric triplets have had the strengths of all three transitions measured.

The level structure of the mirror nuclei ^{38}Ar and ^{38}Ca, $T_3 = 1$ and -1 respectively, below 5 MeV shown in Figure 17 is quite similar. The transition strengths in Weisskopf units of corresponding transitions in the two nuclei are listed in Table III. The first three pairs of strengths listed in Table III, corresponding to the decays of the first and second excited 2^+ states to the 0^+ ground state, and the decay of the first excited 0^+ state to the 2^+ first excited state, are all E2 strengths. The strengths within ^{38}Ar are in the proportion of 3:1.4:1 while in ^{38}Ca they are in the proportion of 2.5:2.7:1. The

Figure 16. The [experimental widths]$^{1/2}$ plotted as a function of T_3. The straight lines are a result of a linear least squares fit. The ratio α for the three sets of data is also given. The data for the mass A = 30 triplet are from (Kuhlmann 1973), the data for the mass A = 34 triplet is from (Caraca 1972) and the data for ^{38}K and ^{38}Ar are from (Hasper 1973, Engmann 1971) and (Engelbertink 1969), respectively.

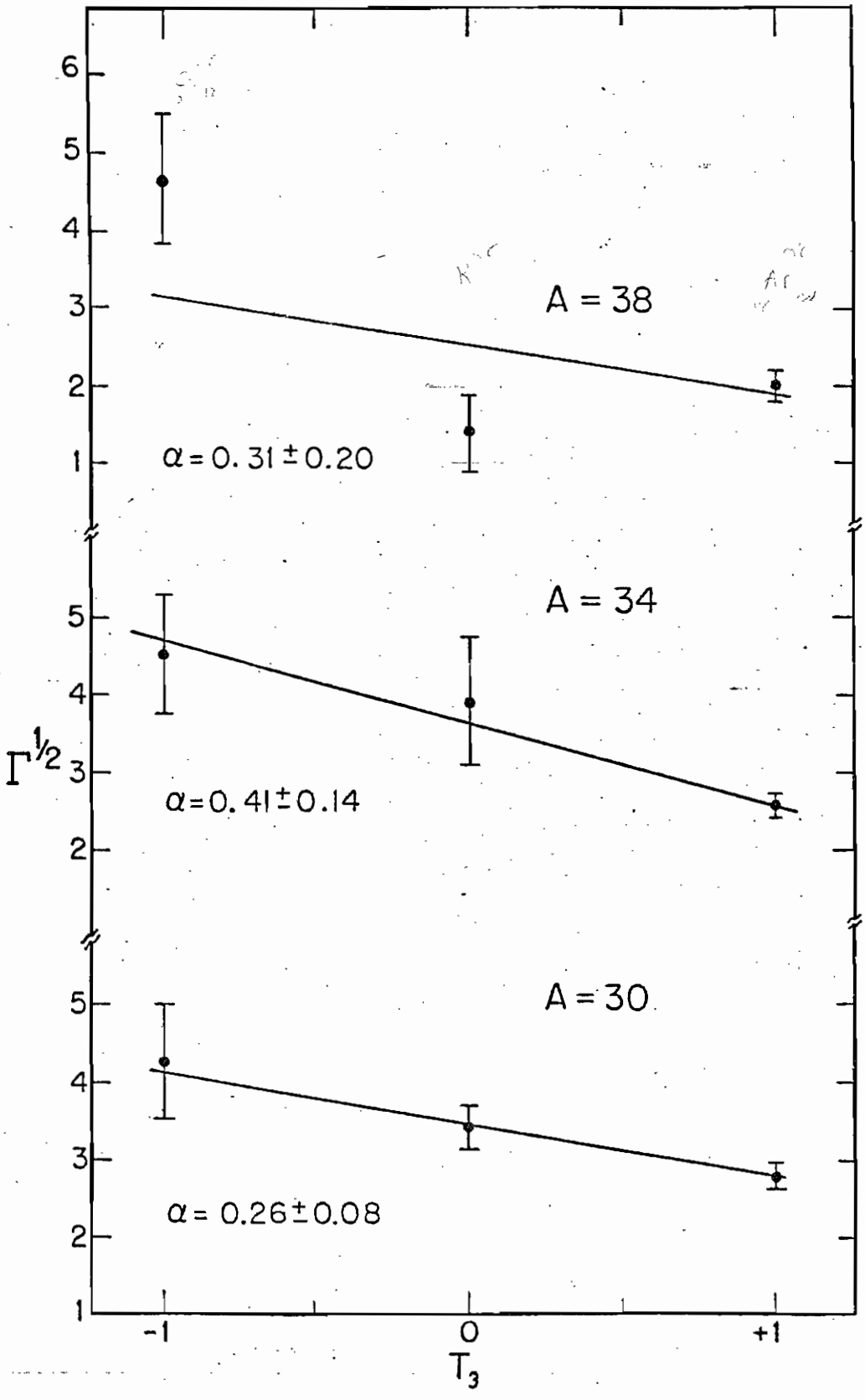
A = 38
α = 0.31 ± 0.20
A = 34
α = 0.41 ± 0.14
A = 30
α = 0.26 ± 0.08
Γ^1/2
T3
-1
0
+1

Figure 17. Experimental energies, spins and parities for the mirror nuclei ^{38}Ca and ^{38}Ar. The data for ^{38}Ar is from Engelbertink, et. al.(1969), except for the lifetime of the 3.377 MeV level, which is from the work of Kern et. al.(1972). The spin and parity assignments for ^{38}Ca are from the work of Davies, et. al.(1967) and Paddock (1971). The level ordering of the 3^- - 2^+ doublet was determined by this study.

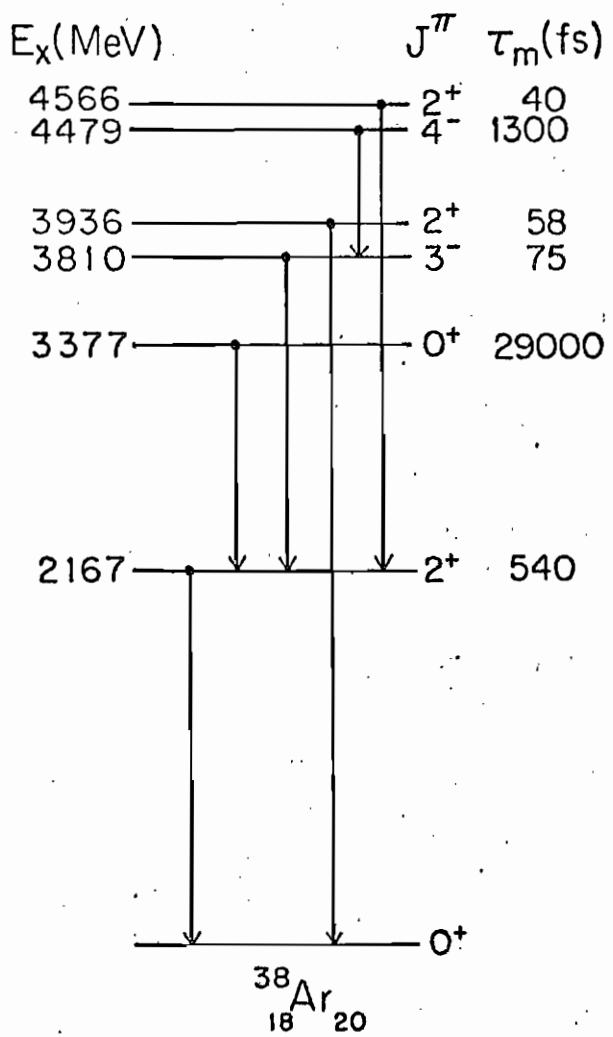
E_x(MeV)
J^π
τ_m(fs)
4566
4479
3936
3810
3377
2167
2^+
4^-
2^+
3^-
0^+
2^+
0^+
40
1300
58
75
29000
540
$^{38}_{18}Ar_{20}$

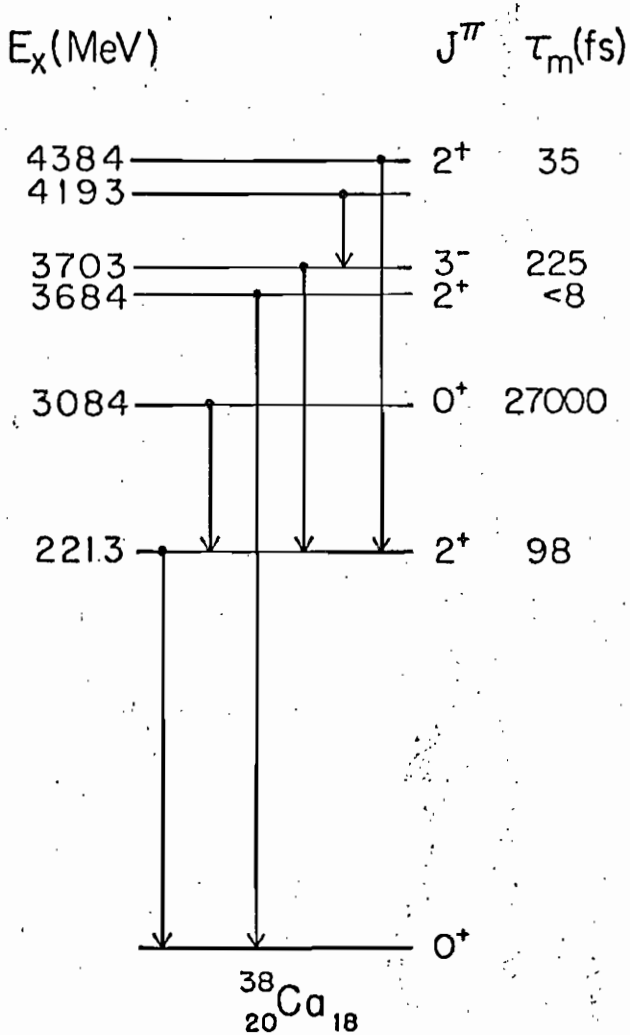
E_x(MeV)
J^π
τ_m(fs)
4384
4193
3703
3684
3084
2213
2^+
3^-
2^+
0^+
2^+
0^+
35
225
<8
27000
98
$^{38}_{20}Ca_{18}$

Table III

The transition strengths of analogous transitions in ^{38}Ar and ^{38}Ca. All transitions are assumed to be pure. The subscripts on the J^{π} values indicate the n^{th} excited state of given spin and parity.

Multipole	$J_i^{\pi} \rightarrow J_f^{\pi}$	$\lvert M(^{38}Ca)\rvert^2$ W.u.	$\lvert M(^{38}Ar)\rvert^2$ W.u.
E2	$2_1^+ \rightarrow 0_{gs}^+$	20.4	4.1
E2	$2_2^+ \rightarrow 0_{gs}^+$	22.6	2.0
E2	$0_1^+ \rightarrow 2_1^+$	8.0	1.4
E1	$3_1^- \rightarrow 2_1^+$	1.2×10^{-3}	2.5×10^{-3}
M1	$2_3^+ \rightarrow 2_1^+$	8.8×10^{-2}	9.6×10^{-2}

next pair of transitions listed correspond to the $\Delta T = 0$, E1 transitions from the 3^- levels to the first excited state. The work of Warburton et. al. (1969) has shown that E1 transitions in mirror nuclei should have equal strengths. In this case they differ by a factor of 2. The rule for M1 transitions is weaker. These transitions, with $\Delta T = 0$, are expected to be about equal in strength if the transitions are of average or stronger than average strength. While the strengths of the M1 transitions in ^{38}Ar and ^{38}Ca are weaker than the average strength of 10^{-1} W.u. reported by Endt et. al.(1974) the rule still works as the strengths only differ by a factor of 1.1.

The Oak Ridge-Rochester shell model (French 1969) was used to calculate the level energies, spins and parities for T = 1 levels in mass 38 nuclei, using the modified surface delta interaction (MSDI) of Glaudemans et. al. (1967). The results of this calculation are compared with the experimental spectra in Figure 18. The MSDI is an outgrowth of the surface delta interaction (SDI). The SDI is defined as

$$V_{SDI}(ij) = -4\pi A_T \delta(\Omega_{ij})\delta(r_i-R)\delta(r_j-R)$$

where Ω_{ij} is the angular coordinate of the two particles i and j. This interaction was capable of accurately reproducing the energy spectrum of a given nucleus. By adding a T-dependant, J-independant term to the SDI, i.e.

$$V_{MSDI} = V_{SDI} + B_T$$

Glaudemans et. al. showed that the agreement of experimental and theoretical binding energies and excitation energies was good over a large range of masses.

The shell model calculation performed in this study used the MSDI two body matrix elements obtained with $[A_T,B_T]$ equal to [0.8,0.6] and [0.6,-1.44] for T = 1 and 0 respectively. The allowed configurations were $(2s_{1/2})^j(1d_{3/2})^k(1f_{7/2})^l(2p_{3/2})^m$ with $j+k+l+m = 10$ and the restrictions that $l+m \leq 2$, $2 \geq j \geq 4$,

Figure 18. Theoretical and experimental level diagram for ^{38}Ca. The theoretical spectrum was calculated with the Oak Ridge-Rochester shell model code using the MSDI.

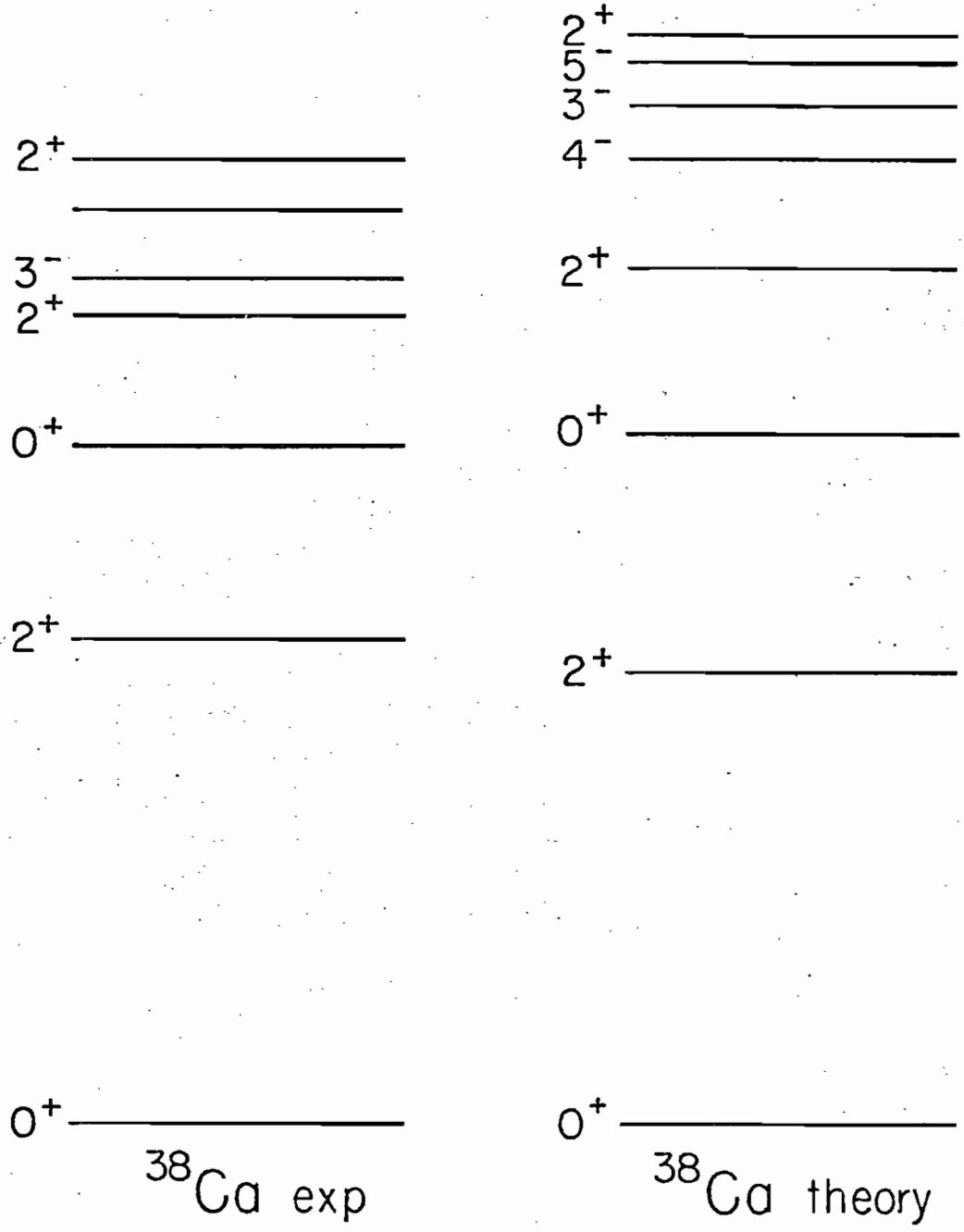
2+
3-
2+
0+
2+
0+
38Ca exp
2+
5-
3-
4-
2+
0+
2+
0+
38Ca theory

and $4 \geq k \geq 8$. Thus the positive parity states are described by pairs of nucleons in any of the four shells and by $(s_{1/2})^3(d_{3/2})^7$ and $(f_{7/2})^1(p_{3/2})^1$ configurations. The negative parity states are described in this model by a single nucleon in either the f or the p shell. Only T = 1 states were calculated with J restricted between 0 and 6 inclusive. The energy differences between the shells were set at 2 MeV. The values for A_T, B_T and the energies of the orbitals are within the range reported in the literature(Glaudemans 1967, Engelbertink 1969)

The level structure shown in Figure 18 agrees well with the experimental level scheme. It should be noted that the first 0^+ level appeared above 6 MeV until pairs of particles were allowed into the f and p shells. This state was missing in all the earlier calculations performed with more restricted configuration spaces(e.g. Engelbertink 1969). The model predicts that the primary configuration of the 0^+ state at 3 MeV is $(s_{1/2})^4(d_{3/2})^4(f_{7/2})^2$ with a very small admixture of $(s_{1/2})^4(d_{3/2})^6$. The ground state is described as $(s_{1/2})^4(d_{3/2})^6$ with some $(s_{1/2})^4(d_{3/2})^4(f_{7/2})^2$. The configuration of the first 2^+ level is primarily $(s_{1/2})^4(d_{3/2})^6$, while the largest component of the second 2^+ state is $(s_{1/2})^4(d_{3/2})^4(f_{7/2})^2$. The third 2^+ level is predicted to be of a complex structure with sd, sdf, sdp and sdfp components. Both of the negative parity states have fairly pure $(s_{1/2})^4(d_{3/2})^5(f_{7/2})^1$ configurations.

The first excited 0^+ state was not observed in the (p,t) experiments of either Davies et. al. (1967) or Paddock (1971). It was populated in this work and that of Shapiro et. al.(1970) both of which used the (^{3}He,n) reaction. The predicted $(f_{7/2})^2$ structure of this state may offer an explaination of the low cross section with the (p,t) reaction and the relatively lower excitation energy (3.08 MeV) in ^{38}Ca to that of ^{38}Ar (3.38 MeV). If it is assumed that two protons must be excited from the $d_{3/2}$ orbital to form this level in ^{38}Ca(and two neutrons must be excited in ^{38}Ar) the ^{40}Ca(p,t)^{38}Ca reaction would not be

able to form this state easily as it picks up a pair of neutrons from the ^{40}Ca target. If the ^{38}Ar 0^+ state is formed with two neutrons in the $f_{7/2}$ shell, while the level in ^{38}Ca is formed with two protons in the $f_{7/2}$ orbital, the coulomb energy of the ^{38}Ca would be lowered relative to the ground state configuration, resulting in the level energy of the 0^+ level in ^{38}Ca being less than the analogous level in ^{38}Ar.

The success of this model is outstanding. It has reproduced the level energies,and their spins and parities quite well. The predicted structure of the states is nowhere in conflict with the experimental data, and where the data allows, e.g. the 0^+ level, the predicted structure can be used to explain the experimentally observed behavior. More work remains to be done as there are no calculated transition probabilities for ^{38}Ca. A comparison of theoretical and experimental strengths would allow a more detailed test of this model.

APPENDIX

The general law describing the rate of decay of an unstable state is:

$$\frac{dN(t)}{dt} = -\lambda N(t) \qquad (1)$$

where λ is the probability of decay and N(t) is the number of nuclei in the state at time t. Equation (1) can be solved for N(t) yielding the well known exponential decay law.

$$N(t) = N(0)e^{-\lambda t} \qquad (2)$$

Now if a state is being populated by another decaying state, as in the case of one excited state decaying by γ-ray emission to another excited state, the change in the instantaneous population of the lower state is

$$dN_1(t)/dt = -\lambda_1 N_1(t) + \lambda_2 N_2(t)$$

thus

$$N_1(t) = N_2(0)\times(\lambda_2/(\lambda_1-\lambda_2))\times(e^{-\lambda_2 t} - e^{-\lambda_1 t}).$$

If the state being fed (state 1) has a non-zero initial population then

$$N_1(t) = N_1(0)e^{-\lambda_1 t} + N_2(0)\left(\frac{\lambda_2}{\lambda_1-\lambda_2}\right)(e^{-\lambda_2 t} - e^{-\lambda_1 t}) \qquad (3)$$

Now, to determine the effect that indirect population will have on the observed attenuation factor, first note that the expression for the attenuation factor of a γ-ray observed at an angle θ, recoiling at an

angle $\phi(t)$ to the beam axis is given by,

$$F(t) = \frac{v(t)}{v(0)} \times \frac{\cos\theta\cos\phi(t)}{\cos\theta} = \frac{v(t)}{v(0)} \cos\phi(t) \equiv V(t) \qquad (4)$$

and thus for a group of recoiling excited nuclei,

$$F(\tau) = \int_0^\infty F(t)R(t)dt \Big/ \int_0^\infty R(t)dt \qquad (5)$$

where R(t) is the decay rate of the state being observed, i.e. $R=-\lambda N$. For a state being populated directly and indirectly by gamma cascade, with initial populations of $N_i(0)$ and probabilities of decay λ_i, the observed attenuation factor is:

$$F_{obs} = \frac{\int_0^\infty [\lambda_1 V_1(t) N_1(0) e^{-\lambda_1 t} + \sum N_i(0) \left(\frac{\lambda_1\lambda_i}{\lambda_1-\lambda_i}\right)(e^{-\lambda_i t} - e^{-\lambda_1 t}) v_i(t)]dt}{\int_0^\infty \lambda_1 N_1(t)dt}$$

which, noting that $\lambda = 1/\tau$, and that $\int_0^\infty \lambda_1 N_1(t)dt = \sum N_i$

$$F_{obs} = \nu_1 F_1(\tau_1) + \sum_{i=2}^{n} \nu_i \frac{\tau_i F_i(\tau_i) - \tau_1 F_i(\tau_1)}{\tau_i - \tau_1}$$

where $\nu_i = N_i/(\sum N_i)$.

LIST OF REFERENCES

K.Alder,A.Bohr,T.Huus,B.Mottelson,A.Winther,Rev.Mod.Phys.28(1956)432

S.E.Arnell,Ark.Fys.26(1963)153

E.Bashandy,Nucl.Instr.Meth.12(1961)227

A.E.Balugrund,Nucl.Phys.88(1966)501

D.C.Camp,G.L.Meredith,Nucl.Phys.A166(1971)349

J.M.G.Caraca,R.D.Gill,B.C.Robertson,I.S.Towner,H.J.Rose,Nucl.Phys. A133(1969)337

W.G.Davies,J.C.Hardy,D.J.Skyrme,D.G.Montague,K.Ramavataram,T.A.Hodges, RHEL/R-156(1967)111

S.Devons,G.Manning,D.St.P.Bunbury,Proc.Phys.Soc.A68(1955)18

D.J.Donahue,R.L.Hershberger,Phys.Rev.C4(1971)1693

P.M.Endt,C.van der Leun,Nucl.Data Tables,13(1974)67

G.A.P.Engelbertink,P.W.M.Glaudemans,Nucl.Phys.A123(1969)225

G.A.P.Engelbertink,G.van Middelkoop,Nucl.Phys.A138(1969)588

R.Engmann,E.Ehrmann,F.Brandolini,C.Signorini,Nucl.Phys.A162(1971)295

B.Fastrup,P.Hvelplund,C.A.Sautter,Mat.Fys.Medd.Dan.Vid.Selsk.35(1966) 10

J.B.French,E.C.Halbert,J.B.McGrory,S.S.M.Wong,Adv.in Nucl.Phys. Vol.3(1969)

P.W.M.Glaudemans,P.J.Brussaard,B.H.Wildenthal,Nucl.Phys.A102(1967)593

P.W.M.Glaudemans,P.M.Endt,A.E.L.Dieperink,Ann.Phys.63(1971)134

E.C.Halbert,J.B.McGrory,B.H.Wildenthal,S.P.Pandya,Adv.in Nucl.Phys. Vol.4 to be published

H.Hasper,P.B.Smith,Phys.Rev.C8(1973)2240

W.Kessel,R.Bass,E.C.Hagen,N.R.Roberson,C.R.Gould,D.R.Tilley, to be published

W.Kessel,R.Bass,R.Wechsung,Nucl.Phys.A206(1973)193

B.D.Kern and P.D.Bond,Nucl.Phys.A181(1972)403

E.Kuhlmann,W.Albrecht and A. Hoffmann, Nucl.Phys.A213(1973)82

J.Lindhard,M.Scharff,H.E.Schiøtt,Kgl.Danske Videnskab.Selskab, Mat.-Fys.Medd.33(1963)No.14

J.Lindhard,M.Scharff,Phys.Rev.124(1961)128

J.H.Ormrod,J.R.McDonald,H.E.Duckworth,Can.J.Phys.43(1965)275

R.A.Paddock,Phys.Rev. C5(1971)485

P.B.Parks,H.W.Newson,R.M.Williamson,Rev.Sci.Instr.29(1958)834

C.E.Ragan,Ph.D.Dissertation,unpublished(1970)

E.Selin,S.E.Arnell,O.Almen,Nucl.Instr.Meth.56(1967)218

M.H.Shapiro,C.Moss,W.M.Denny,Nucl.Phys.A128(1969)73

M.H.Shapiro,A.Adams,C.Moss,W.M.Denny,Nucl.Phys.A144(1970)17

S.J.Skorka,J.Hertel,T.W.Retz-Schmidt,Nucl.Data A2(1966)347

L.D.Skouras,Phys.Lett.31B(1970)439

E.K.Warburton,J.W.Olness,A.R.Poletti,Phys.Rev.160(1967)938

E.K.Warburton,J.Weneser,Isospin in Nuclear Physics,ed.by D.H. Wilkinson(North-Holland,Amsterdam,1969)

B.H.Wildenthal,E.C.Halbert,J.B.McGrory,T.T.S.Kuo,Phys.Rev.C4(1971)1266

B.H.Wildenthal,E.Newman,NuclPhys.A118(1968)347

BIOGRAPHY

Edward Christopher Hagen

Date of Birth: 29 September 1944

Place of Birth: Washington, D.C.

Colleges Attended:

Wesleyan University			
Boston University	B.S.	physics	1968
Duke University	Ph.D.	physics	1974

Publications: Lifetimes of Low-Lying Levels in ^{57}Ni(with C.R.Gould, R.V.Poore,N.R.Roberson,G.E.Mitchell and D.R.Tilley) Phys.Rev.Lett.25(1970)463

Lifetime measurements in ^{27}Si(with C.R.Gould,N.R.Roberson, and D.R.Tilley) Particles and Nuclei 2(1972)92

Study of Excited States in ^{39}Ca and ^{39}K(with W.Kessel, R.Bass,N.R.Roberson,C.R.Gould and D.R.Tilley) to be published 1974

Abstracts: Lifetime Measurements of Low-Lying States in ^{27}Si (with C.R.Gould,N.R.Roberson,and D.R.Tilley) Bull.Am. Phys.Soc.16(1971)491

Study of the Gamma Decays of ^{51}Ti from the ^{50}Ti(d,pγ)^{51}Ti and ^{48}Ca(α,nγ)^{51}Ti Reactions(with G.P.Lamaze,C.R.Gould and N.R.Roberson)Bull.Am.Phys.Soc.17(1972)582

Lifetimes of Low-Lying Levels in ^{38}Ca(with N.R.Roberson and D.R.Tilley)Bull.Am.Phys.Soc. to be published

Positions Held: Teaching Assistant, Duke University, 1968-1969

Research Assistant, Duke University, 1969-1974